January 2022

Inelastic Behaviour Of Thin-Walled Circular Steel Tubular Columns Under Pushover And Cyclic Loading

Njiru J. Mwaura

INELASTIC BEHAVIOUR OF THIN-WALLED CIRCULAR STEEL TUBULAR COLUMNS UNDER PUSHOVER AND CYCLIC LOADING

By

Njiru Mwaura, M.S.

A Thesis
Submitted to the Graduate Faculty

of the

UNIVERSITY OF NORTH DAKOTA

In partial fulfillment of the requirements

for the degree of

Master of Science
Civil Engineering
College of Engineering and Mines

Grand Forks, North Dakota

May
2022

This thesis, submitted by Njiru Mwaura in partial fulfillment of the requirements for the Degree for Master of Science in Civil Engineering from the University of North Dakota, has been read by the Faculty Advisory Committee under whom the work has been done and is hereby approved.

_____

Iraj Mamaghani

_____

Daba Gedafa

_____

Cai Xia Yang

This thesis is being submitted by the appointed advisory committee as having met all the requirements of the School of Graduate Studies at the University of North Dakota and is hereby approved.

_____

Chris Nelson
Associate Dean, School of Graduate Studies.

_____

Date

PERMISSION

Title: Inelastic behavior of thin-walled circular steel tubular columns under pushover and cyclic loading

Department: Civil Engineering

Degree: Master of Science (MSc.)

In presenting this thesis in partial fulfillment of the requirements for a graduate degree from the University of North Dakota, I agree that the Library of this University shall make it freely available for inspection. I further agree that permission for extensive copying for scholarly purposes may be granted by the professor who supervised my thesis work or, in his absence, by the Chairperson of the department or the dean of the School of Graduate Studies. It is understood that any copying or publication or other use of this thesis or part thereof for financial gain shall not be allowed without my written permission. It is also understood that due recognition shall be given to me and to the University of North Dakota in any scholarly use which may be made of any material in my thesis.

Njiru Mwaura

05/03/22

TABLE OF CONTENTS

LIST OF TABLES

LIST OF EQUATIONS

LIST OF FIGURES

NOMENCLATURE

TWST	Thin-walled steel tubes
FEM	Finite Element Modelling
TWCSTC	Thin-walled circular steel tubular column
MPC	Multi point control
H_y	Horizontal lateral load
δ_y	Initial displacement
H_{max}	Maximum strength
$H_{0.9}$	Post buckling strength (90% of H_{max})
δ_m	Deformation at maximum strength
$\delta_{0.9}$	Deformation at post buckling strength
R_t	Local buckling of the column section parameter
λ	Global buckling of the column parameter

ACKNOWLEDGMENTS

First, I express my deepest appreciation to my academic and research advisor Dr. Iraj Mamaghani for his guidance and help throughout my research. He offered the knowledge and relevant experience required in this research and has excellently mentored me in this area of specialization. I would like to express my special thanks and highest appreciation to my MSc. committee; Dr. Daba Gedafa, Dr. Cai Xia Yang, and the Graduate Director Dr. Yeo Lim for their support and help.

Next, I would like to appreciate the University of North Dakota for making it possible for me to do research and giving me the opportunities and facilities needed. Also, I would like to thank friends and colleagues from the Civil Engineering department and other departments as well.

Finally, I would like to appreciate all my family members. A special thanks to my wife, Penina and my parents; Njiru and Ruth for their prayers and moral support. Despite the distance, they have always shown love and mental support all through. Lastly, I would like to thank our little children, Mutugi, Rosalind and Nadine for their love and patience. I am very grateful to them and their contribution to my life.

DEDICATION

To my wife

Penina Njiru

and my parents

Njiru Karigi and Ruth Runji

and my son and daughters

Tesla Mutugi, Rosalind Marie Curie and Nadine

ABSTRACT

Thin-walled circular steel tubular columns have been used as bridge piers widely around the globe because of their excellent seismic performance: ductility, strength, and energy dissipation capacity. This thesis investigates the inelastic behavior of thin-walled circular steel tubular columns with a uniform section and thin-walled circular steel columns with diaphragms. The loading protocol considered for this study is either pushover or cyclic lateral loading in the presence of a constant axial load. The effects of a pushover and cyclic lateral loading on the behavior of the thin-walled circular steel tubular bridge piers have been evaluated through analysis of failure mode, hysteresis curve, envelope curve, stiffness and strength degradation characteristic, and energy-dissipating capacity, including interaction effects of local buckling and flexural buckling, and post-buckling regimes. The analysis applies the finite element model (FEM) that considers the effect of both material and geometric nonlinearities. Also, in this research a comprehensive parametric study was carried out to investigate the effects of the key design parameters and namely are: the radius to thickness parameter (R_t), the column slenderness ratio parameter (λ), and the magnitude of axial load (P/P_y). Finally, a series of proposed formulae for strength and ductility evaluation for thin-walled circular steel tubular columns are given.

CHAPTER 1

INTRODUCTION AND BACKGROUND

1.1 Introduction

Architects and engineers keep on improving the aesthetic and structural components of buildings, bridges and tunnels (Watanabe et al., 2000). These structures are designed to cope with many prevailing environmental conditions, such as high winds and earthquakes. An earthquake produces the most extreme seismic conditions and the structures are designed to resist them with no failure. A design is considered successful if these structures continue being safe and offering the intended comfort to all the occupants after these events.

The ability of a steel structure to withstand extreme seismic loading conditions without collapse is influenced by the energy dissipation capacity and the ductility of the material used to build the structure. For example, rollers are very effective structural components used as energy dissipaters in bridges and offshore structures through inelastic action.

Thin-walled circular steel tubular bridge piers, with and without longitudinal and lateral stiffeners, in the form of cantilever columns and planar rigid frames, have been used in modern highway bridge systems because of their high strength and torsional rigidity. For example, Figure 1, shows bridge piers of thin-walled circular and rectangular box sections supporting an elevated highway bridge in Nagoya, Japan (Mamaghani et al., 2008). These structures experience damage caused by local buckling, global buckling or an interaction of both. Local buckling is characterized by a large width-to-thickness ratio of the flange plate (for the box section), and by a large radius-to-thickness ratio of the circular section. Those parameters are in Figure 1.

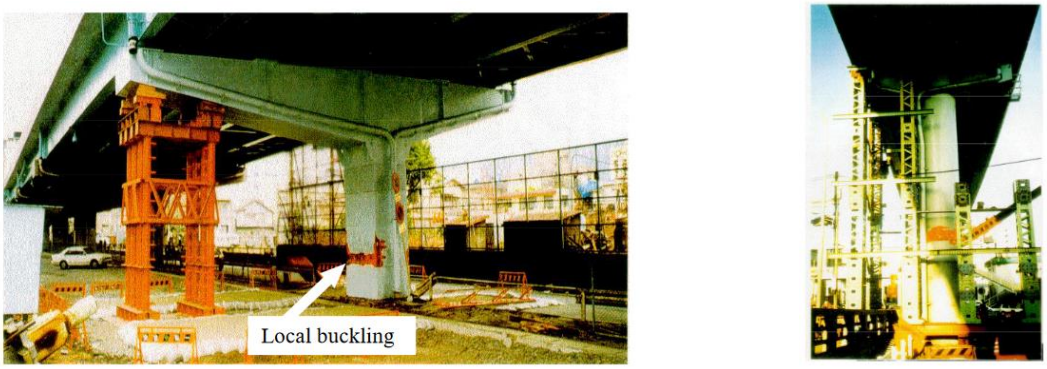

(a) Local buckling (rectangular section) (b) Local buckling (circular section)

Figure 1: Bridge piers, which suffered severe local buckling damage in the Kobe Earthquake, 1995 (Mamaghani, 2006).

Figure 1 indicates the effects of the Kobe earthquakes on various bridges in Japan after the Kobe earthquake in 1995. The figure shows occurrence of local buckling on bridge piers due to inelastic behavior and severe earthquake as shown on the thin walled tubular columns. The Kobe earthquake was assigned a magnitude of 7.2 by the Japan Meteorological Agency (JMA) and the epicenter was located approximately 20 km South-West of the Kobe city (Esper & Tachibana, 1996). It destroyed many elevated roadways and since then Kobe earthquake has inspired researchers to investigate the strength and ductility of thin walled tubular columns and their impact to prevent the collapse of bridges during strong earthquakes.

Researchers have been conducting experiments and studies on applications of thin-walled tubular steel columns and the advantages they have in earthquake prone areas (Al-Kaseasbeh and Mamaghani, 2018, 2019; Goto et al 2020; Ucak and Tsopelas, 2014). Thin walled tubular steel columns possess valuable advantages compared to conventional ones made of reinforced concrete. Thin-walled steel tubular columns are more efficient due to their light weight, high strength, ductility, and ease and speed of construction, especially, when limited construction space is needed (Mamaghani, 1996)

Research including both experimental and numerical analyses have been conducted to identify methods that improve the strength and ductile behavior of the thin-walled steel columns under

constant axial force and cyclic lateral loading (Usami and Ge, 1998; Goto et al, 1998, Mustafa et al., 2016). Observations on thin-walled steel tubular columns after major earthquakes have shown their vulnerability to local buckling, global buckling and an interaction of both.

This study aims to numerically analyze thin-walled circular steel tubular columns with diaphragms in an attempt to improve the ultimate strength, ductility, energy absorption, and post-buckling behavior of a uniform thin-walled circular steel tubular columns. To achieve this goal, uniform thin-walled circular steel tubular columns were numerically analyzed under a constant axial and pushover/cyclic lateral loading. The accuracy of the adopted FEM has been verified based on experimental results in the literature. The study results indicate that thin-walled circular steel tubular columns with diaphragms show significant improvements in ultimate strength, ductility, energy absorption and post-buckling behavior as compared to their counterpart uniform thin-walled circular steel tubular columns.

The main reason for the improved behavior of the thin-walled circular steel tubular column (TWCSTC) with diaphragms is their ability to mitigate the buckling near the base of the column where the buckling most likely occurs. Also, a parametric study was carried out to assess the key effects of key design parameters on the strength, ductility and energy dissipation of both uniform columns and columns with diaphragms. These key design parameters and namely are: the radius to thickness parameter (R_t), the column slenderness ratio parameter (λ), and the magnitude of axial load (P/P_y). Finally, a series of design formulae to predict strength and ductility evaluation for thin-walled circular steel tubular columns are given. The proposed formulae are expected to be applied in the improvement of steel design and fabrication manuals for cost-effective approaches.

1.2 Problem Statement

Thin-walled circular steel tubular columns are prone to damage or collapse due to interaction of both local buckling parameter of the column section (R_t) and the slenderness ratio parameter

of the column (λ). Large horizontal lateral load caused by extreme earthquake loads greatly increases the above mentioned design parameters. In order to mitigate the effect of large pushover and cyclic lateral loads there is a need to study the inelastic behavior of thin-walled circular steel tubular columns under a constant axial load and any of these horizontal lateral loading. In addition, interaction equations that relate these key design parameters need to be developed. The interaction equations enables practical application in the design of thin-walled circular steel tubular columns considering both safe and cost effective design.

1.3 Research Objectives

There have been investigations on thin-walled steel tubular columns modelling bridge piers within the last two decades. Researchers have studied both circular and square box sections under a constant axial load and a uni/multidirectional cyclic lateral loading. These studies established that thin-walled steel tubular columns experience local buckling near the base in a range equivalent to the diameter or the width of the circular and square box columns respectively (Al-Kaseasbeh & Mamaghani, 2019, Mamaghani, 1996). In order, to solve this problem and improve strength and ductility of thin-walled steel columns, two diaphragms are fitted within the column and investigated. The diaphragms are located at a distance between $2D_0$ and $3D_0$ respectively. In addition, the study concludes that thin-walled steel tubular columns with diaphragms exhibit enhanced strength and ductility under both pushover and cyclic loading. Moreover, these columns reduces local buckling occurrence and absorbs more energy during severe earthquakes.

This research aims to investigate the interaction of local buckling and flexural buckling on the strength and ductility of thin-walled steel tubular columns. First, the results of experiments conducted in Japan were used to substantiate the accuracy of the finite element modeling (FEM) using ABAQUS/Standard version 6.14 adopted in this study. The thin-walled steel

tubular columns were evaluated for strength, ductility, energy absorption and post buckling under constant axial load, pushover and unidirectional cyclic lateral loading.

1.4 Methodology

In order to achieve this goal, three tested thin-walled steel tubular columns which were circular, reported in the literature (Goto et al., 1998, 2014), were numerically analyzed under a constant axial load, pushover or unidirectional cyclic lateral loading to validate the accuracy of the adopted FEM model.

Then, a comprehensive parametric study of twenty columns was conducted. These thin-walled steel tubular columns were proposed by assigning key design parameters that include: the radius to thickness ratio parameter of the column cross-section (R_t), column slenderness ratio parameter (λ), and the magnitude of axial load (P/P_y). The study also aims to determine the appropriate ranges of these key design parameters.

Finally, a series of design equations using the interaction of R_t, λ and P/P_y to predict the strength and ductility of the thin-walled steel tubular columns with diaphragms were developed. Strength and ductility improvement achieved from diaphragms was investigated.

1.5 Organization of the Thesis

This thesis consists of six chapters as shown in Fig. 2. Chapter 1 gives a general introduction about buckling problems on thin-walled circular steel tubular columns and various studies conducted to explore the problem. It also includes problem statement and the objectives of the research. Chapter 2 deals with the Literature review on numerical analysis and inelastic behavior of thin-walled circular steel tubular columns under a constant axial load, pushover or unidirectional cyclic lateral loading. Chapter 3 describes the inelastic behavior of prismatic thin-walled circular steel tubular columns under a constant axial load, pushover or unidirectional cyclic lateral loading. The test data from the literature and the numerical analysis has well been described.

Chapter 4 describes the inelastic behavior of the prismatic thin-walled circular steel tubular columns with diaphragms under a constant axial load, pushover or unidirectional cyclic lateral loading. In addition, it includes a comprehensive parametric study using the key design parameters that include R_t, λ and P/P_y. Chapter 5 describes the analysis and results for the parametric study and the description of the design equations developed from the analysis. Finally, the conclusions and the recommendations are summarized in Chapter 6.

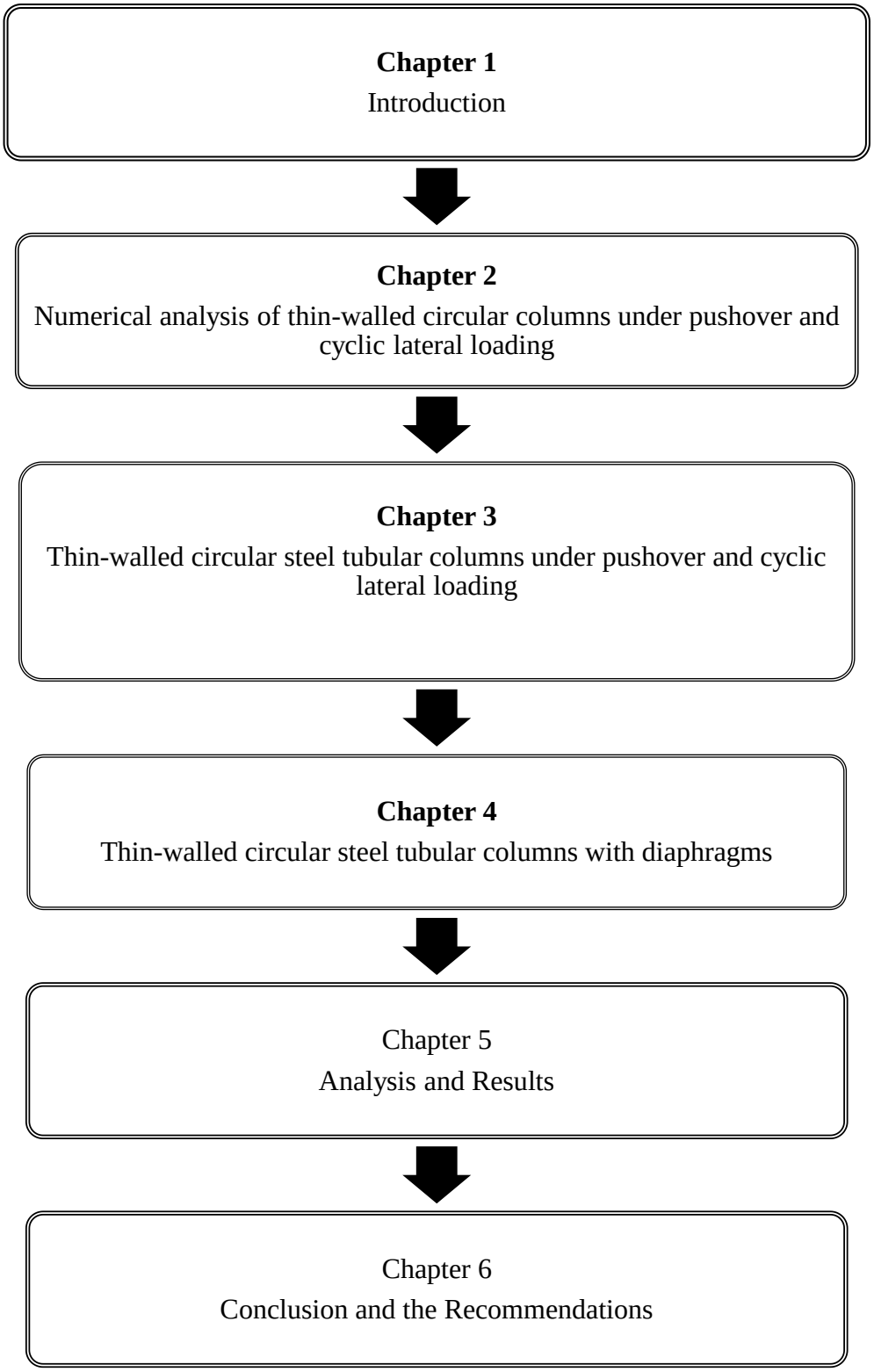

Figure 2: Organization of the Thesis

CHAPTER 2

NUMERICAL ANALYSIS OF THIN-WALLED CIRCULAR STEEL COLUMNS UNDER PUSHOVER AND CYCLIC LATERAL LOADING.

2.1 Introduction

Bridge piers and columns in buildings have predominantly been constructed of structural steel (Watanabe et al., 2000). Accurate numerical models are necessary to evaluate the seismic performance and loading bearing mechanism of thin-walled steel tubular columns (Li et al., 2017).

Thin-walled circular steel tubular columns with fixed base as illustrated in Fig 3 have widely been used in Japan as piers of highway bridges (Lyu et al., 2020, Serras et al., 2016 and Mamaghani et al., 1997). Numerical simulations of the performance of thin-walled steel tubular columns under a constant axial load and a cyclic lateral loading on thin-walled circular tubes to improve strength and ductility have been investigated (Ge et al., 2000, Aoki & Susantha, 2005, Fukumoto et al., 2003, and Al-Kaseasbeh & Mamaghani, 2019).

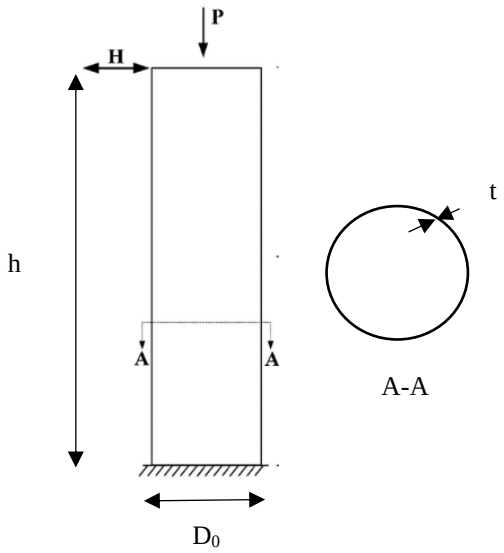

Figure 3: Cantilevered column section (longitudinal and cross-section)

2.2 Key design parameters of Thin-Walled Circular Steel Tubular Columns

Thin-walled circular steel tubes are vulnerable to damage from local buckling, global buckling or an interaction between both (Al-Kaseasbeh & Mamaghani, 2019a). Local buckling occurs near the column base at a height equal to the diameter of the column (Mamaghani & Packer, 2002).

The buckling of the constituent plates may have caused a sudden decrease of bearing capacity in the lateral direction after the peak strength resulting in reduced energy dissipation, and also deterioration of the bearing capacity in the vertical direction. The strength and ductility of thin-walled circular steel tubes are affected by the radius to thickness ratio parameter (R_t) of the cross-section and slenderness ratio (λ) of the columns (Mustafa et al., 2018 and Kwon et al., 2007). R_t controls the local buckling behavior of the plate, while λ has a considerable effect on the global stability of the column (Mamaghani, 2008, Goto et al., 1998). For any tested columns, definitions of R_t, λ and P/P_y parameters are given as follows in equations 2.1-2.3 (Dalia et al., 2021 and Lyu et al., 2020):

$$0.06 \leq R_t = \frac{D_0 \sigma_y}{2 t_s E_s} \sqrt{3(1 - v_s^2)} \leq 0.12 \qquad (2.1)$$

$$0.25 \leq \lambda = \frac{1}{\pi}\sqrt{\frac{\sigma_y}{E_s}}\frac{2h}{r_s} \leq 0.6 \quad (2.2)$$

$$0.05 \leq \frac{P}{P_y} \leq 0.2 \quad (2.3)$$

Where:

D_0 = diameter of the thin walled circular steel tubular column (mm)

t = thickness of the thin walled circular steel tubular column (mm)

r_s = radius of gyration (mm)

A_s = cross-sectional area (mm^2)

σ_y = yield stress (N/mm^2)

E_s = Young's modulus (N/mm^2)

ν_s = Poison's ratio

h = height of the column (mm)

P = compressive load acting at the top of the columns (KN)

P_y= yield compressive load. (KN)

2.3 Finite Element Modelling of Thin-Walled Circular Steel Tubular Columns under Pushover or Cyclic Lateral Loading.

2.3.1 Material behavior

The inelastic behavior of thin-walled steel structures is dependent on mechanical property observed in the stress-strain relationship. Pushover and cyclic lateral loading is modelled under different material models which are available in various FEM software. The FEM utilizes Von Mises yield criterion and its related flow criterion (Li et al., 2017). Von Mises introduced the

knowledge of yield surface and has been vital during design consideration that includes plasticity in structural steel. The yield surface forms with progression of loading in structures made of structural steel. Increase in loading beyond the yield surface results in plastic deformation characterized by irreversible changes on the surface of the structural steel. Inelastic behavior of steel during loading can be described using material hardening rules. The main material hardening rules are; isotropic hardening rule and is described in Fig. 4 (a and b) and bilinear/multi-linear kinematic hardening rule (see Fig. 4 (c and d) are commonly utilized due to their availability within FEM software. Isotropic hardening material model considers strain hardening taking place in both tension and compression directions at equal values due to cyclic loading. It doesn't not fully account for the plasticity of steel since it does not include Bauschinger effect (reduction of yield surface in one direction, either tension or compression due to plastic deformation under cyclic loading. In contrast, the kinematic hardening rule considers the Bauschinger effect, and the yield surface with a constant radius translates. The yield surface translation results in strain-hardening of the material in loading direction and softening of the material in opposite (unloading) direction. In this research, the multilinear kinematic hardening material model is used in the analysis as it predicts material behavior better than the isotropic hardening material model (Gao et al., 2000).

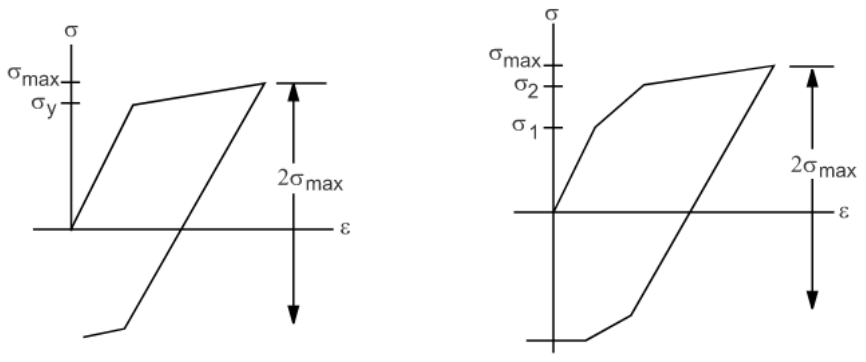

(a) (b)

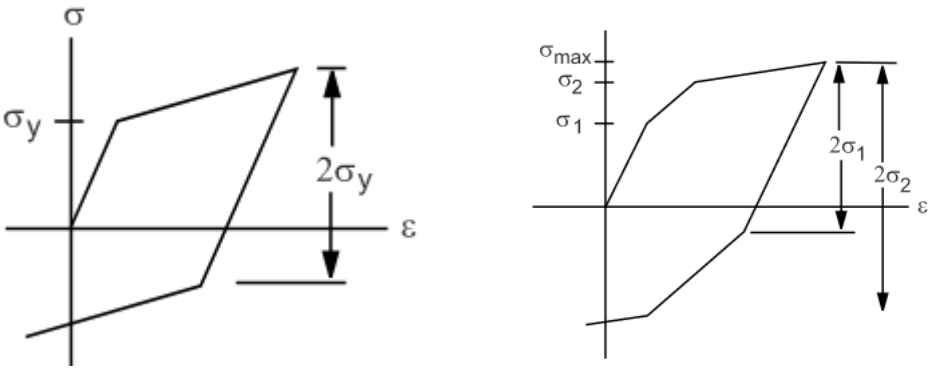

(c) (d)

Figure 4: Material hardening model (a) bilinear isotropic, (b) multi-linear isotropic (c) bilinear kinematic, (d) multi-linear kinematic (Hibbit & Sorensen, 2014).

2.3.2 Constant axial loading

The thin-walled circular steel tubular columns modelling bridge piers are modelled with presence of a constant axial force (P) as shown in Fig.3. This force is a vertical load applied at the center of the column for this research. However, the same load can be applied eccentrically depending with the nature of the load application. In reality, load (P) accounts for service loads (dead and live loads) that act on the column during its life time.

2.3.3 Finite element meshing of thin-walled circular tubular columns

Meshing considers first the choice of the geometric discretization shapes that are efficient and saves computation time. Thin-walled steel tubular columns are divided into parts, and each part is meshed in consideration to quick convergence of the solution. In this research, the columns are divided into two parts. The lower part which is discretized using shell element is further divided into two parts and its lower bottom part (equivalent to the diameter of the tube) is finely meshed compared to the other part. The upper part is discretized as a beam element and considers a coarse mesh. The shell element denoted as SR4 in Abaqus documentation, uses a 4 node reduction integration shell element. In addition, it also utilizes Gaussian integration point (5 points) across its cross-section to distribute plasticity (Hibbit & Sorensen, 2014). The

beam element, denoted as B31 considers two nodes at every discretization region in one dimension and its consideration makes computation faster due to its simplicity.

2.3.4 Loading Path

In presence of a constant axial load, a horizontal lateral load is considered to stimulate maximum effect on strength and ductility of bridge piers. This load is applied as a displacement on the top part of the column. Depending on whether the loading protocol is pushover or cyclic lateral loading the post buckling behavior that simulates maximum deterioration of the column is monitored. The pushover loading considers one large displacement applied monotonically while the cyclic lateral load considers either unidirectional or bidirectional loading cases where initial displacement is increased in multiples and in alternate directions.

CHAPTER 3

THIN-WALLED CIRCULAR STEEL TUBULAR COLUMNS UNDER PUSHOVER AND CYCLIC LATERAL LOADING.

3.1 Experimentally tested and modeled thin-walled circular steel tubular columns

Conventional prismatic thin-walled circular tubular steel columns under combined axial and pushover/cyclic loading experience premature buckling behavior, either local buckling near the base of the column or global buckling on overall column. Under this buckling behavior, circular columns are unable to fully utilize their strength and ductility capacities. To overcome these limitations, thin-walled circular tubular steel columns with diaphragms is proposed as alternatives to uniform TWCSTC. The diaphragms are made of the same structural material as the thin-walled circular tubes and are located at heights equal to $2D_0$ and $3D_0$. This diaphragm configuration was chosen due to its ability to eliminate local buckling at the base of the column. Table 1 shows material and geometric properties of the uniform TWCSTC and uniform TWCSTC with diaphragms. Table 1 shows the material, geometric properties and the magnitude of loading for all the analyzed columns.

Table 1: Geometric, Material properties and initial displacement of the analyzed columns.

Column	**h (mm)**	**D_0 (mm)**	**t (mm)**	**P/P_y**	**σ_y (Mpa)**	**σ_u (Mpa)**	**E (GPa)**	**H_y (kN)**	**δ_y (mm)**	**R_t**	**λ**
P5-e0	4391	891	8.4	0.15	235	426	206	232	14	0.10	0.3
P1	3403	891	9	0.12	289.6	510	206	415.2	10.6	0.11	0.26
C column	3403	900	9	0.124	298.6	495	206	414.9	10.6	0.12	0.26

All columns are loaded with one-cycle at each displacement (N = 1),

$P_y = \sigma_y * A$, $A = \pi (D_0^2 - D_i^2)/4$, $D_i = D_0 - 2t$, t = thickness of plate for the column.

I = moment of inertia = $\pi (D_0^4 - D_i^4)/64$, S = elastic section modulus = $\pi (D_0^4 - D_i^4)/32D_0$

D_0 = Outer diameter of the tube, D_i = Inner diameter of the tube

3.2 Finite Element Modelling

Finite element (FE) analyses on the pushover/cyclic behavior of TWCSTC were carried out using the commercial finite element software, Abaqus/Standard version 6.14 (Hibbit & Sorensen, 2014).

3.2.1 Comparative experimental specimens

The experiments conducted in Japan (Goto et al., 1998, 2014; Kazuhiro Nishikawa et al., 1998) are used to substantiate the accuracy of the finite element modelling (FEM) using ABAQUS/Standard version 6.14 adopted in this study.

The thin-walled steel tubular columns are evaluated for strength, ductility, energy absorption and post-buckling under constant axial load, pushover or unidirectional cyclic lateral loading to validate the accuracy of the adopted FEM model.

The columns modeled bridge piers, and are tested as cantilever columns under a constant axial load and each is subjected to different lateral load history. Fig. 5 (a) shows the column geometry and Fig. 5 (c) shows the column cross-section.

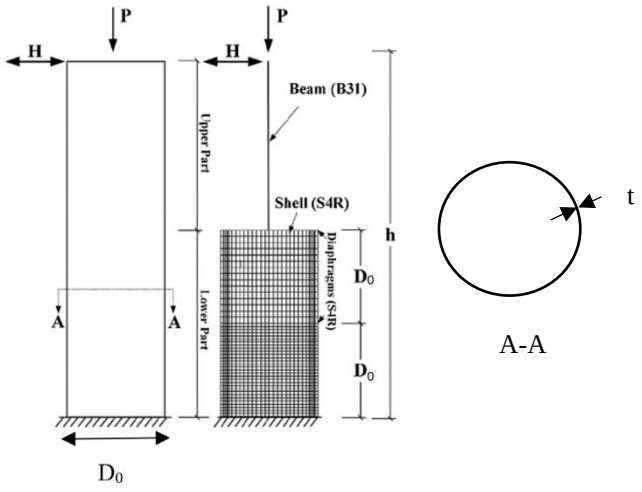

(a) (b) (c)

Figure 5: Column model (a) Column (b) FE Meshing (c) Cross-Section A-A

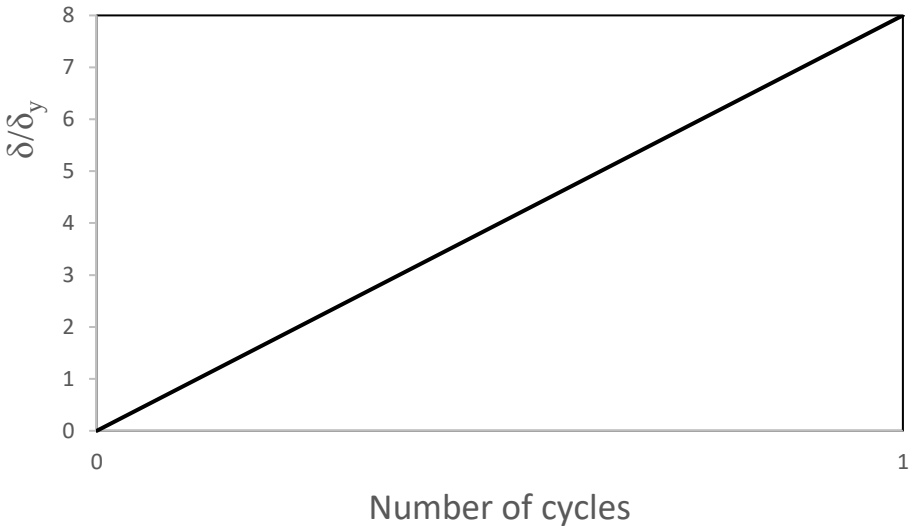

Figure 6: Pushover loading path protocol

Figure 7: Cyclic loading path protocol

3.2.2 Material Model

The adopted FEM utilized the material model available within the commercial software, Abaqus/Standard version 6.14. In this study, the linear kinematic hardening model in the ABAQUS program was chosen. This FEM employing a kinematic hardening model was used to simulate the inelastic behavior of thin-walled steel tubular columns of circular cross-section subjected to pushover and cyclic lateral loading in the presence of constant axial load.

3.2.3 FEM meshing

FEM analysis was conducted using commercial finite element software, Abaqus/Standard version 6.14 (Hibbit & Sorensen, 2014). Figure 5 (b) indicates the meshing sizes for height equivalent to D_0 and the entire column. The column was modeled as a shell element SR4 for the height equal to $2D_0$. S4R is a four-node shell element with reduced integration. A beam-column element (B31) was adopted for the upper part *(h-2D₀)*. The interface between the S4R and B31 elements has been modeled using multi-point constraint (MPC). Analytical efficiency was improved by dividing the TWCSTC columns into sections; the lower part of the thin-walled circular steel column (equal to the diameter of the tube, D_0) meshed to S4R elements of size 20mm and another D_0 on top of the lower part meshed to S4R elements of size 40mm. The upper part of the column ($h-2D_0$) was considered as a beam-column was divided into B31 elements with a dimension of 100mm. The mesh sizes stated above were decided by trial and error and the displacement convergence criterion for this analysis considered a convergence tolerance of 10^{-5} and 300 iterations. The initial geometrical imperfection and residual stresses were neglected for this analysis as previous studies indicated that they have negligible effect on cyclic behavior of analyzed columns (Al-Kaseasbeh & Mamaghani, 2019b).

3.2.4 Support condition

The support condition was considered as a cantilevered column fixed at the base.

3.2.5 Loading protocol

3.2.5.1 Pushover loading protocol

The pushover loading protocol shown in Fig. 6 considers a large displacement applied monotonically in one direction. This research considered a maximum displacement of $8\delta_y$ which coincided with the final displacement for the cyclic lateral loading.

3.2.5.2 Cyclic loading protocol

The displacement-controlled cyclic loading protocol was employed in this study as shown in Fig. 7. The solid wavy line denotes one-cycle loading path (N = 1). A fully reversed displacement controlled unidirectional alternate load is applied to the top of the columns under a constant compressive load P. The amplitude of the alternate load is assumed to increase by δ_y in a stepwise manner after one cycle of loading.

The initial yield displacement δ_y and horizontal lateral load is given by equations 3.1 and 3.2 respectively (Ucak & Tsopelas, 2012):

$$\delta_y = \frac{H_y h^3}{E_s I_s} \tag{3.1}$$

$$H_y = (\sigma_y - \frac{P}{A_s}) \frac{Z_s}{h} \tag{3.2}$$

In Equations. (3.1) and (3.2): H_y, E_sI_s, A_s and Z_s denote the lateral yield force, bending rigidity, cross-section area, and section modulus, respectively, of a cantilevered hollow steel tube with a fixed base. The yield displacements and lateral yield loads for all analyzed columns are listed in Table 1.

3.3 Comparison of Analysis and Test Results

This section presents, the computed normalized lateral load versus lateral displacement hysteresis and envelope curves for the tested columns (P5-e0, P1 and C). The accuracy of the employed FEM has been substantiated using experimental results that were obtained from Japan (Goto et al., 1998; Kazuhiro Nishikawa et al., 1998). Table 2; lists strength and ductility results for the analyzed columns.

Table 2: Strength and ductility of the validated tubular columns.

Column		**Strength and Ductility Ratio (Cyclic)**				**Strength and Ductility Ratio (Pushover)**			
		H_{max}/H_y	$H_{0.9}/H_y$	δ_m/δ_y	$\delta_{0.9}/\delta_y$	H_{max}/H_y	$H_{0.9}/H_y$	δ_m/δ_y	$\delta_{0.9}/\delta_y$
P5-e0	Analysis	1.461	1.315	1.906	3	1.461	1.315	1.906	3
	Test	1.461	1.315	1.906	3	1.461	1.315	1.906	3
P1	Analysis	1.454	1.309	2.4	2.9	1.454	1.31	2.4	3
	Test	1.454	1.309	2.4	2.9	1.41	1.27	2.4	2.9
C	Analysis	1.454	1.309	2.4	3.1	1.454	1.309	2.4	3.9
	Test	1.454	1.309	2.4	3.1	1.454	1.309	2.4	3.9

3.3.1 Pushover behavior

These curves were developed by giving the columns one large displacement ($8\delta_y$). The experiment and the FE analysis exhibited a close agreement. Figures 8, 9 and 10 compare the normalized lateral load versus lateral displacement envelope curves of the columns (P5-e0, P1 and C) obtained from the analysis and experiment under the one-cycle lateral displacement history (see Fig. 6). The solid line denotes numerical results, while the dashed line stands for the experimental results. H_y and δ_y denote the lateral yield load and the corresponding lateral yield displacement respectively.

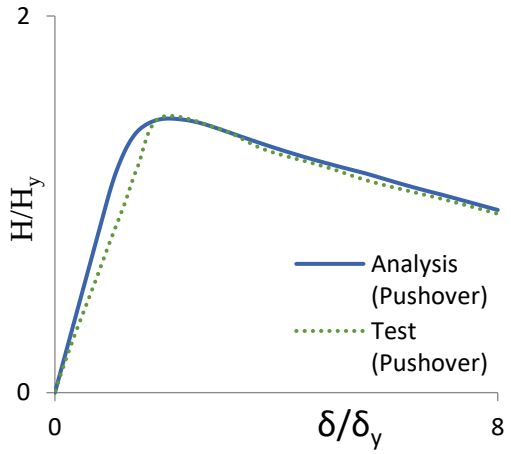

Figure 8: Pushover curve for Column P5-e0

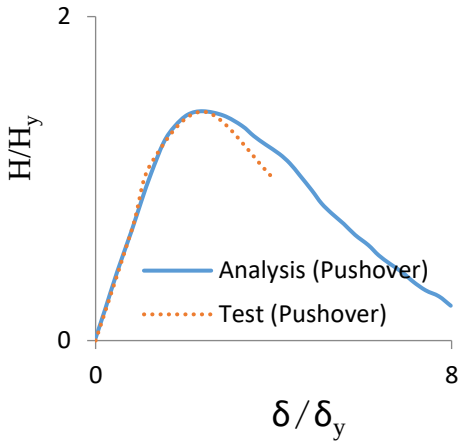

Figure 9: Pushover curve for Column P1

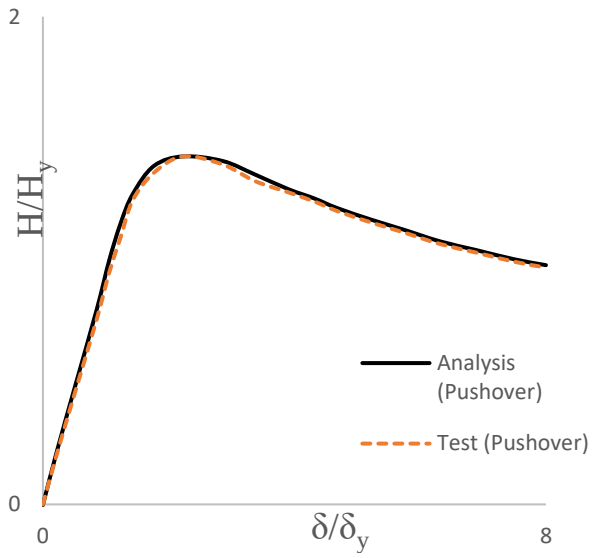

Figure 10: Pushover curve for Column C

3.3.2 Hysteresis behavior

Figures 11, 12, and 13 compare the normalized lateral load versus lateral displacement hysteresis curves of the columns (P5-e0, P1 and C). The solid line denotes numerical results, while the dashed line stands for the experimental results. H_y and δ_y denote the lateral yield load and the corresponding lateral yield displacement, respectively. As shown in the figures, there is a good match between the experimental and analytical results. Referring to Table 2, the FEM predicts the ultimate strength of the uniform TWCSTC with less than a 3% error. This indicates that FE analysis, using the considered geometric and material model captured the structural behavior of TWCSTC with regard to local buckling.

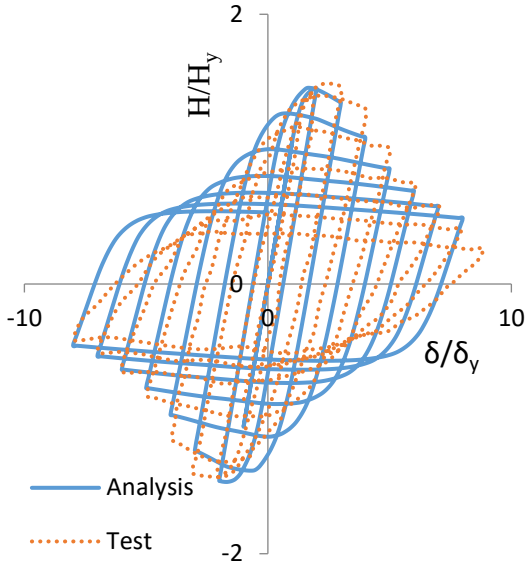

Figure 11: Hysteresis loop for Column P5-e0

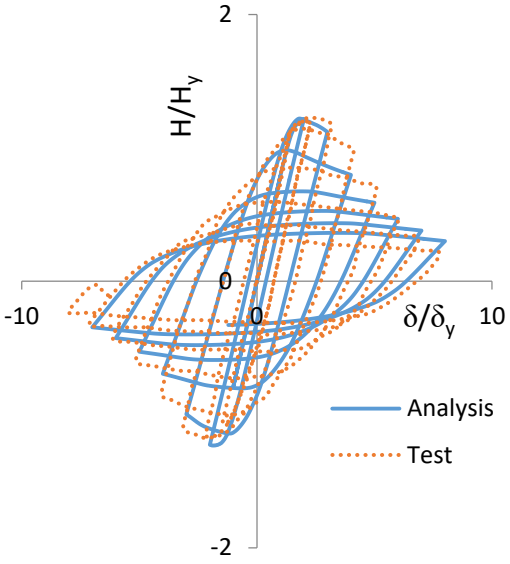

Figure 12: Hysteresis loop for Column P1

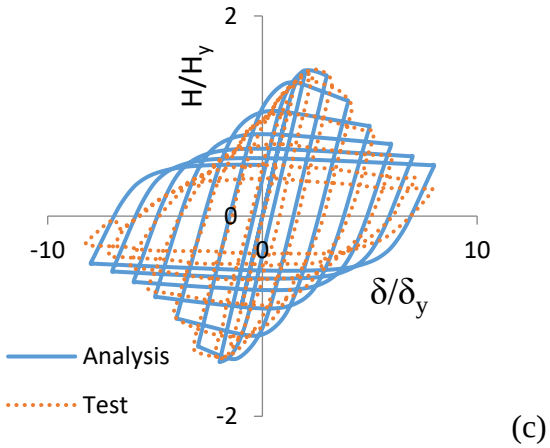

(c)

Figure 13: Hysteresis loop for Column C

3.3.2.1 Buckling mode of column C

Inspection of Figures 14 (a) and (b) show close agreement of numerically obtained buckling shapes and experimental ones. The FEM model accurately captures the ultimate lateral load, deformation capacity and strength degradation. The elephant budge at the base of the column after the formation of the plastic hinge and the final deformed shape for both experimental and numerical models were in good agreement. A comparison of the experimental deformation with FEM failure mode shows a similarity of global plate buckling mode with a half-sine wave. The location and the height of the buckled part were exactly the same for the test and analysis.

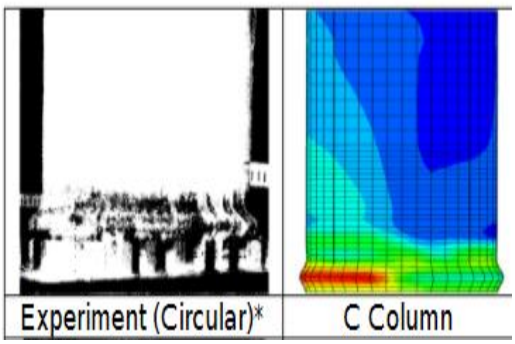

(a) (b)

Figure 14: Buckling at the base of column C (a) Experiment (b) FEM

3.3.3 Envelope curve on hysteresis behavior

The envelope curves were developed from the hysteresis loops above by determining the peak strengths on all whole number amplitudes. Figures 15, 16 and 17 show a close agreement of all envelope curves for both the test and the FE analysis.

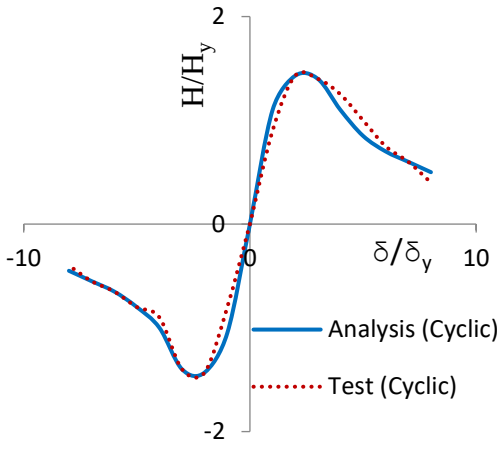

Figure 15: Envelope curve for Column P5-e0

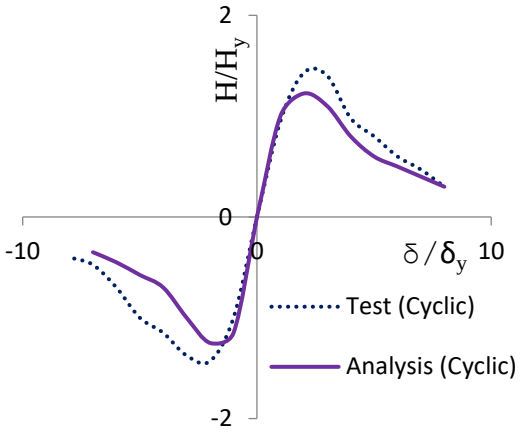

Figure 16: Envelope curve for Column P1

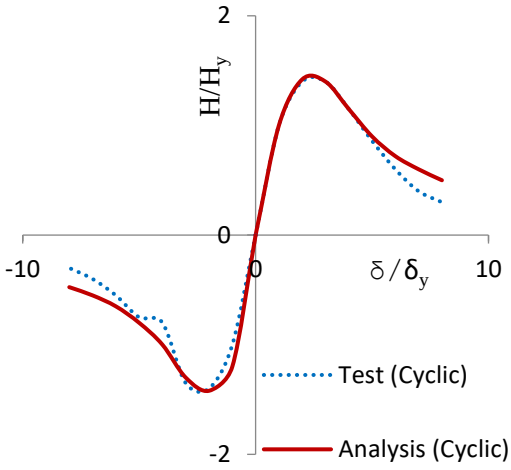

Figure 17: Envelope curve for Column C

3.3.4 Comparative envelope curves

The envelope curves from hysteresis loops and pushover curves were compared. Figures 18, 19 and 20 show the values of maximum strength and post-buckling strength for the columns for the two loading protocols.

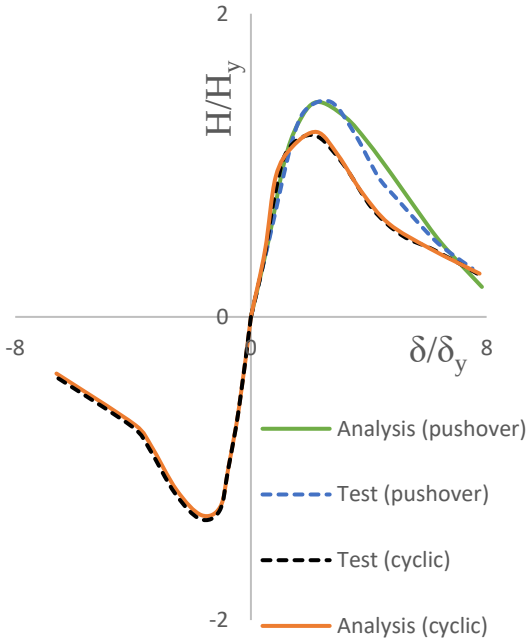

Figure 18: Comparative curves for Column P5-e05

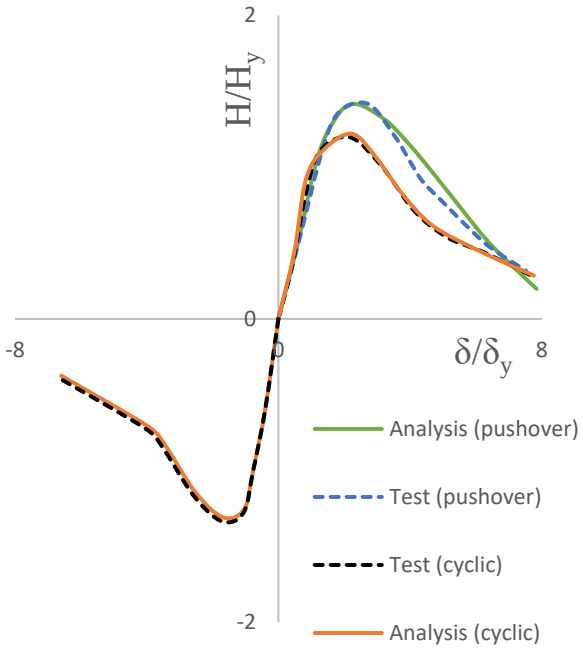

Figure 19: Comparative curves for Column P1

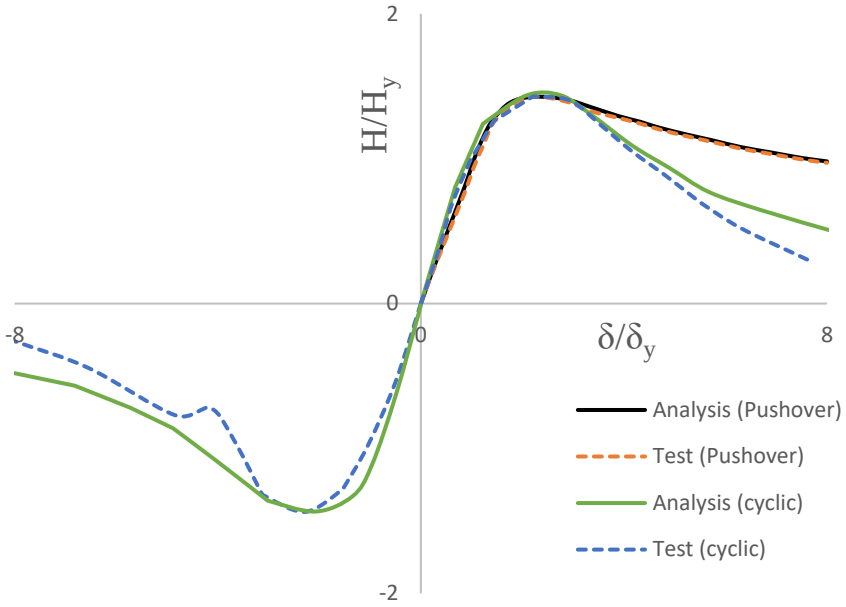

Figure 20: Comparative curves for Column C

3.4 Energy Absorption Capacity

Strength is the capacity of a structure to bear or carry loads, and ductility is the ability of structures to undergo large deformations while maintaining the strength. In this research, energy was determined and calculated as dissipated energy in both cyclic loading and pushover loading. The energy absorption capacity of column has been studied and a normalized energy (E) is defined by equation 3.3 (Al-Kaseasbeh & Mamaghani, 2019b; Mamaghani, 1996).

$$E = \frac{H_y \sigma_y}{2} \sum_{i=1}^{n} E_i \qquad (3.3)$$

In Equation 3.3, E_i = Absorbed energy in i-th half-cycle and n = number of half cycles. (one half-cycle is defined from any zero-lateral load to the subsequent zero-lateral load). Using Eq. (3.3), Figures 21 (a), 21 (b) and 21 (c) compare the normalized cumulative energy absorption vs. n, obtained from the experiment and analysis of the analyzed columns. The normalized energy absorption curves against a number of half-cycles (n) obtained from the analysis fit very

close to the experimental results. Column C dissipated more energy compared to P1 and P5-e0. In addition, pushover loading analysis was carried out and results are shown in Figure 21 (d). Pushover loading dissipated less energy compared to cyclic loading. This is attributed to the fact that pushover loading entailed one large displacement in one direction while cyclic loading involved several cycles with increasing amplitude.

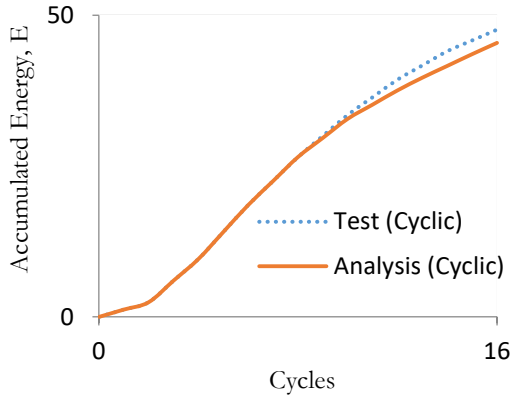

(a)

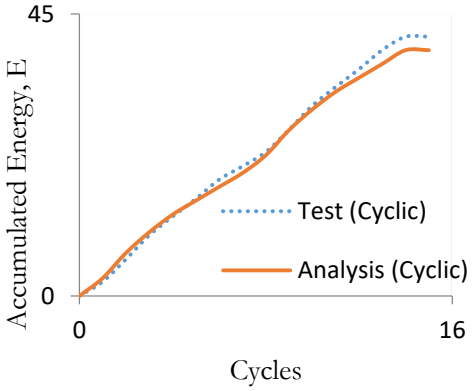

(b)

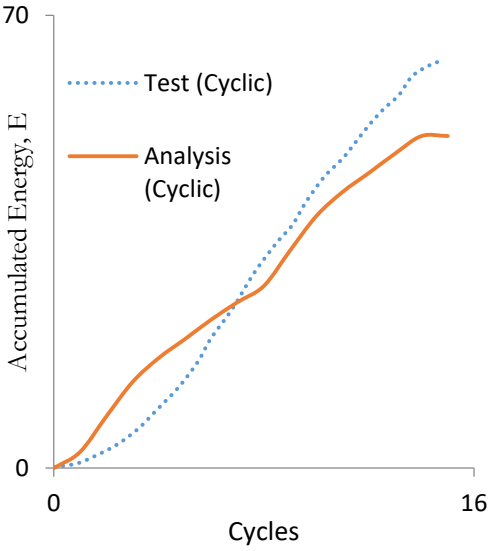

(c)

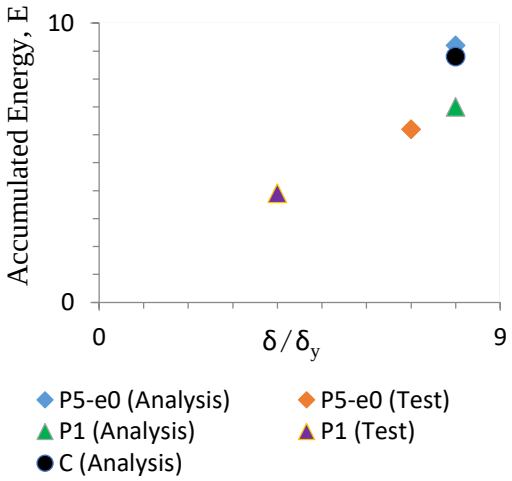

(d)

Figure 21: cyclic lateral loading energy (a) Column P5-e0, (b) Column P1, (c) Column C, (d) Pushover energy for the columns.

3.5 Summary

The envelope curves from the pushover loading and cyclic lateral loading exactly matched and there was noted discrepancies past the post-buckling point due to the sudden reduction in strength and difficult to match in real testing.

The energy curves for the columns P5-e0 and P1 had close agreement when both FEM and test were compared. However, column C had significant variations when the two data sets were compared. This could have been caused by the errors during the experiment or other errors resulting from input displacement.

In conclusion this results confirm the accuracy of the kinematic hardening model in modelling both the pushover and the cyclic behavior of the thin-walled steel tubular columns.

CHAPTER 4.

THIN-WALLED CIRCULAR STEEL TUBULAR COLUMNS WITH DIAPHRAGMS

4.1 Introduction

This chapter discusses the concept meant to improve both the strength and the ductility of the prismatic thin-walled steel tubular columns by inclusion of two diaphragms near the location susceptible to buckling. Addition of diaphragms increases both the strength and the ductility by 12% and 30% respectively.

4.2 The Specimen

The diaphragms are made of the same structural material as the thin-walled circular steel tubular columns and are located at heights equal to $2D_0$ and $3D_0$ as shown in Figure 22. These diaphragms configuration was chosen due to its ability to eliminate or reduce local buckling at the base of the column.

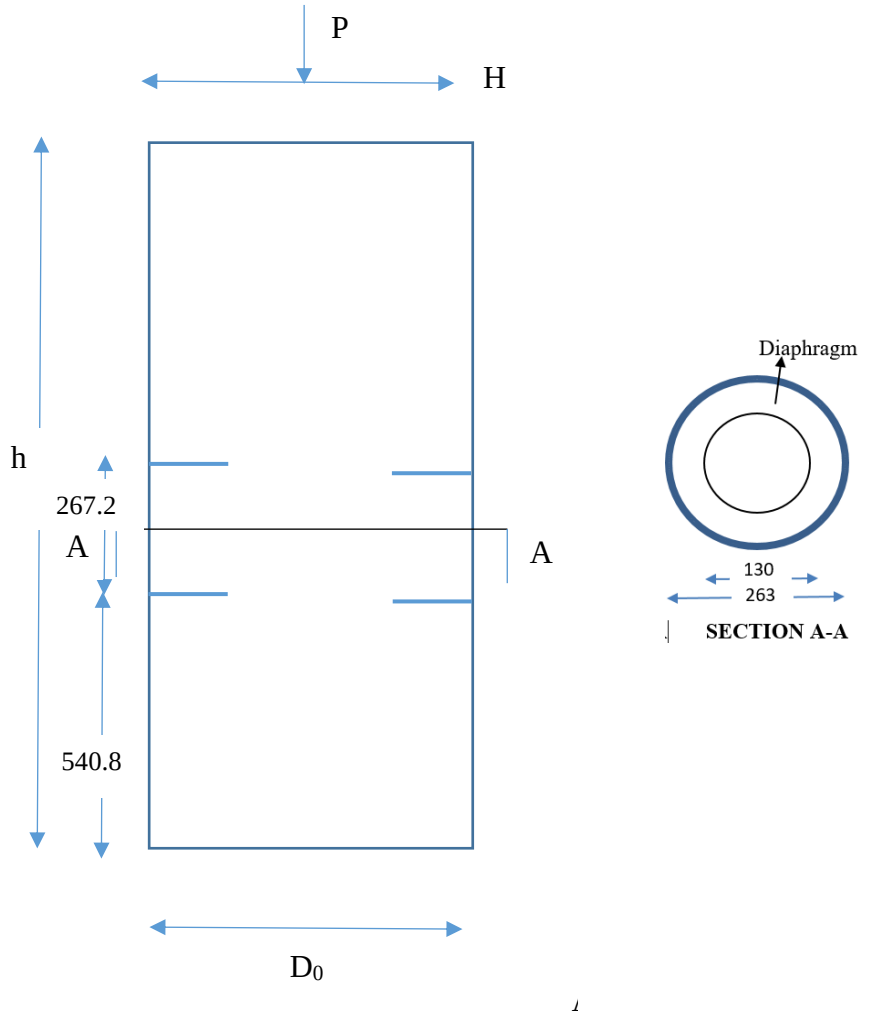

(a) Column with diaphragm (b) Cross-section of the column

Figure 22: Column with diaphragm model (a) Column (b) Cross-section of the column with diaphragm

4.3 FE model validation using experimental data

Figure 23 compares the normalized lateral load versus lateral displacement hysteric curve of the column using the test results (Goto et al., 2014) and the FE analysis results. The lateral displacements exactly matched and there was a slight deviation on strength values between analysis and experimental. It was also noted that the FE model slightly underestimated the lateral strength. This underestimation can be attributed to the second order effects arising due to the specimen-rigid floor interaction. The analysis were carried out with rigid floor assumption and possible foundation interaction effects were not explicitly accounted for. In

addition, there could have existed some experimentation errors especially in the set-up and were not accounted for and reported by the technical team.

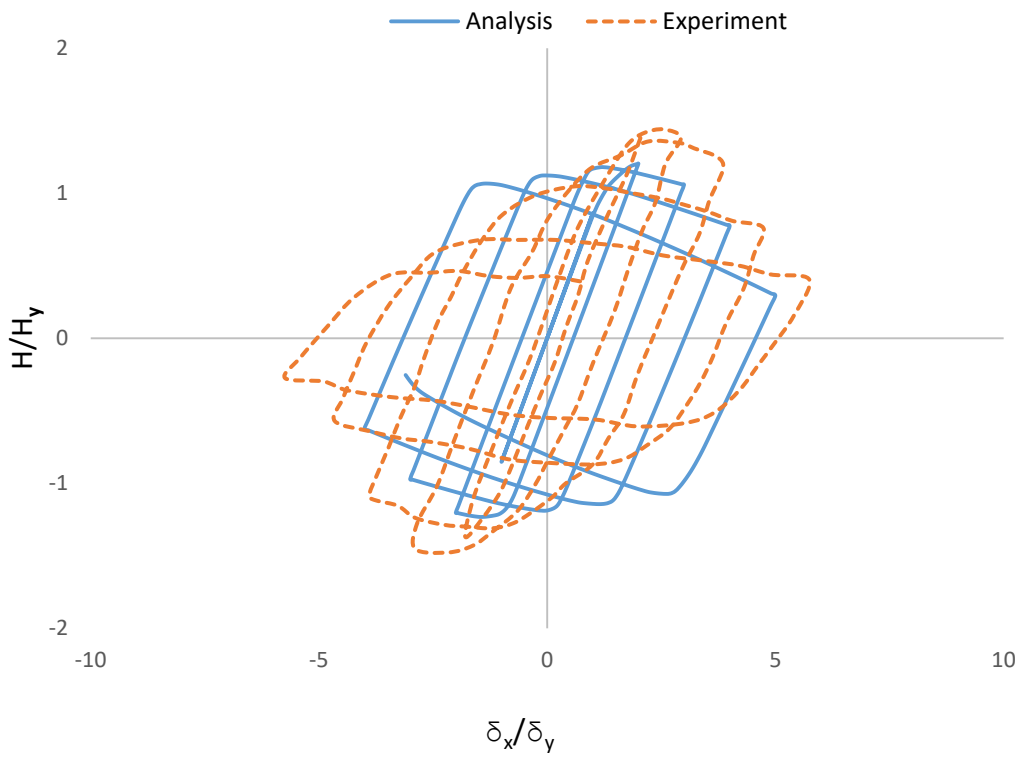

Figure 23: Model validation of the prismatic TWCSTC with diaphragms

4.4 Comparison of a prismatic TWCSTC and a prismatic TWCSTC with diaphragms

Strength and ductility of a prismatic TWCSTC and prismatic TWCSTC with diaphragms were compared. Figures 24, 25, and 26 show comparison of buckled shape, deformation and strength respectively.

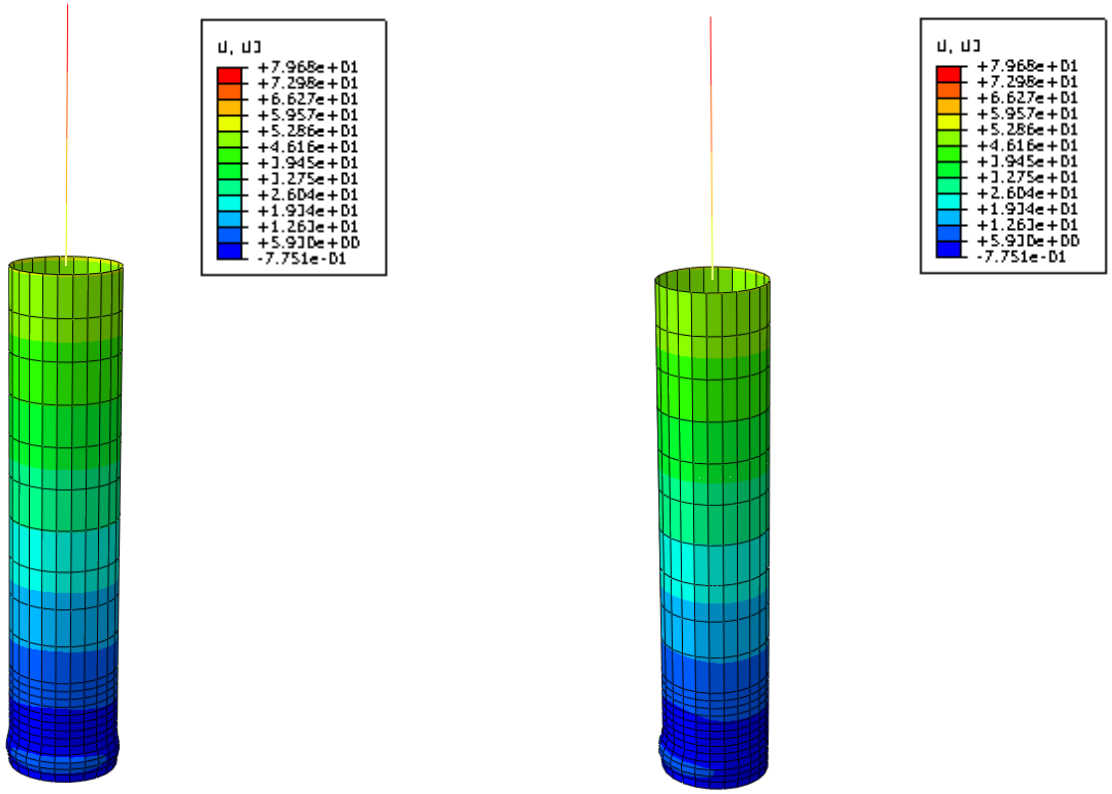

(a) Prismatic TWCSTC (b) Prismatic TWCSTC with diaphragms

Figure 24: Comparison of local buckling shape near the base

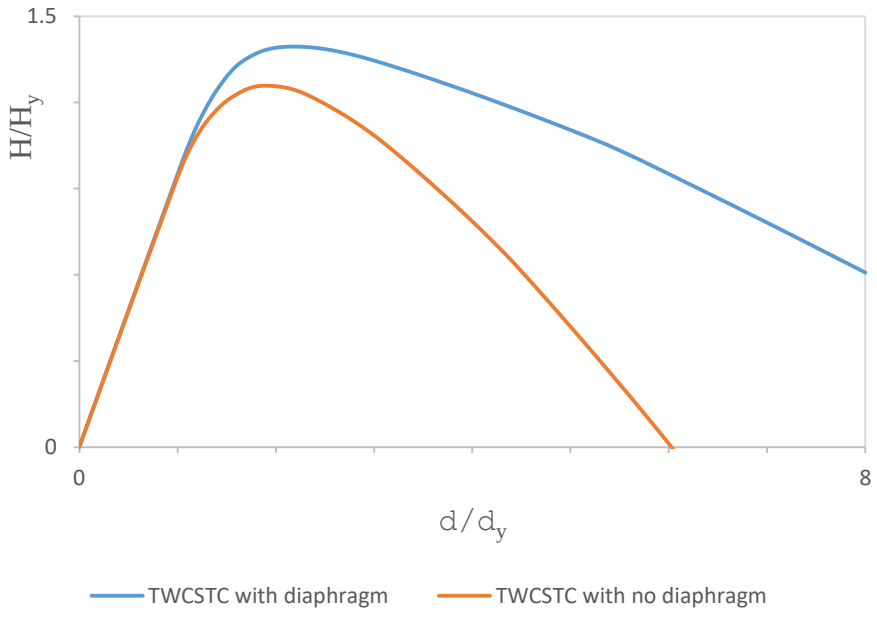

Figure 25: Envelope curve showing improvement in strength and ductility

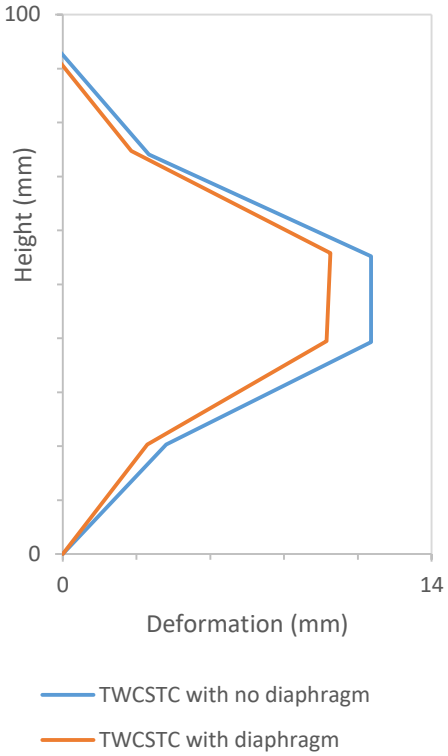

Figure 26: Buckling reduction near the base

4.5 Discussion

Figure 24 show the buckled shapes of a TWCSTC without and with diaphragms respectively. This was the column that was used in the parametric study and the figure confirms reduction of buckling deformation after addition of the diaphragms.

Figure 25 confirms the impact of diaphragms and there was increase in both strength and ductility of the column. The maximum strength increased by 12% while the maximum deformation increased by 30%.

In addition, Figure 26 show the reduction of local buckling after including the diaphragms.

4.6 Parametric Study

A comprehensive parametric study was conducted to provide insight into the effect of key design parameters for the thin-walled circular steel tubular columns including: radius to thickness ratio parameter (R_t), column slenderness ratio parameter (λ) and axial load (P/P_y). The practical range of these parameters in the design of circular bridge piers are: $0.06 < R_t < 0.12$, $0.25 < \lambda < 0.6$, and $P/P_y < 0.2$ (Lyu et al., 2020) and Mamaghani, 1996). In this study, a total of 20 columns listed in Table 3, were analyzed using FEM in Abaqus commercial software. These columns were categorized into two groups and group 1 columns were labelled from C-S-000 to C-S-08 and had a constant R_t of 0.09 and λ values ranging from 0.1 to 0.8. Group 2 columns were labelled from C-R-01 to C-R-10 and had a constant λ of 0.45 and R_t values ranging from 0.05 to 0.14. The constant value was proposed as a mid-point value of generally proposed ranges in previous researches and the varying variable was proposed in between and slightly outside values in Equations 2.1 and 2.2.

Table 3: Geometric properties of analyzed columns.

Column	**h (mm)**	**D_0 (mm)**	**t (mm)**	**R_t**	**λ**	**P/P_y**
Prismatic TWCSTC						
P5-e0 - tested	4391.00	891.00	8.40	0.10	0.30	0.15
P1 - tested	3403.00	891.00	9.00	0.11	0.26	0.12
C column - tested	3403.00	900.00	9.00	0.12	0.26	0.124
Prismatic TWCSTC with diaphragms						
C-S-000	347.05	263.00	4.14	0.09	0.1	0.15
C-S-00	694.10	263.00	4.14	0.09	0.2	0.15
C-S-01	867.63	263.00	4.14	0.09	0.25	0.15
C-S-02	1041.15	263.00	4.14	0.09	0.3	0.15
C-S-03	1214.68	263.00	4.14	0.09	0.35	0.15
C-S-04	1388.20	263.00	4.14	0.09	0.4	0.15
C-S-04A	1561.73	263.00	4.14	0.09	0.45	0.15
C-S-05	1735.25	263.00	4.14	0.09	0.5	0.15
C-S-06	2082.30	263.00	4.14	0.09	0.6	0.15
C-S-07	2429.35	263.00	4.14	0.09	0.7	0.15
C-S-08	2776.40	263.00	4.14	0.09	0.8	0.15
C-R-01	1542.19	263.00	7.46	0.05	0.45	0.15
C-R-02	1549.48	263.00	6.22	0.06	0.45	0.15
C-R-03	1554.72	263.00	5.33	0.07	0.45	0.15
C-R-04	1558.65	263.00	4.66	0.08	0.45	0.15
C-R-05	1561.73	263.00	4.14	0.09	0.45	0.15
C-R-06	1564.19	263.00	3.73	0.10	0.45	0.15
C-R-07	1566.20	263.00	3.39	0.11	0.45	0.15
C-R-08	1567.89	263.00	3.11	0.12	0.45	0.15
C-R-09	1569.31	263.00	2.87	0.13	0.45	0.15
C-R-10	1570.53	263.00	2.66	0.14	0.45	0.15

4.7 Summary.

Table 3 shows the columns sized for the parametric study. The first ten (10) columns which are named from C-S-000 to C-S-08 had a constant R_t of 0.09 and λ ranging from 0.1 to 0.8. The remaining columns named from C-R-01 to C-R-10 had a constant λ of 0.45 and their R_t ranged from 0.05 to 0.14. The above table further indicates the influence of both R_t and λ on the geometry of the columns. For group 1 columns, the height increased as λ increased as thickness remained constant while for group two height increased and thickness reduced as R_t increased.

CHAPTER 5.

ANALYSIS AND RESULTS

5.1 Effect of radius to thickness ratio parameter (R_t)

The effect of the R_t on the strength and ductility of the columns was investigated. The increase in R_t as shown in Table 3 was either due to an increase in the column height or a decrease in the thickness of the cross-section. In this study, the diameter was kept constant and both thicknesses of the cross-section and the height of the columns were varied for all the analyzed columns. The normalized lateral load vs. lateral displacement envelope curves from pushover loading are represented as shown in Figure 27. The normalized ultimate strength (H/H_y) and normalized maximum displacement corresponding to ultimate strength (δ_m/δ_y) increased with a decreasing R_t, increasing thickness and reducing the height. The ultimate strength (H/H_y) improved by 10% as R_t decreased from 0.12 to 0.06 and 1% for the R_t values above 0.12. In addition, maximum displacement corresponding to maximum strength (δ_m/δ_y) increased by 40% (shifted from 0.57 to 0.80), as R_t decreased from 0.12 to 0.06.

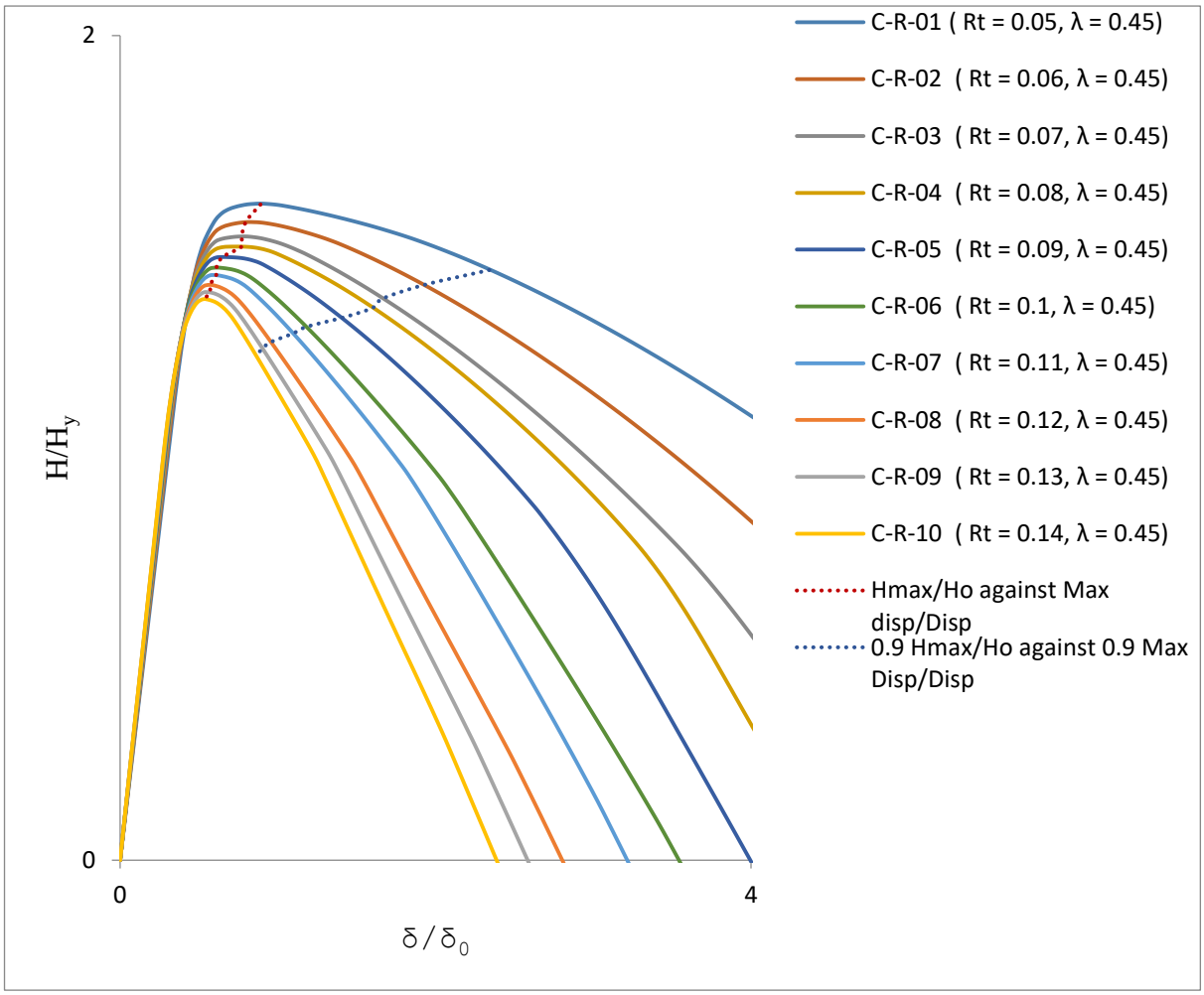

Figure 27: Effect of R_t on strength and ductility on circular tubes with diaphragms.

5.2 Effect of slenderness ratio parameter (λ)

The effect of the λ was studied for the circular columns with diaphragms. H_{max}/H_y and δ_m/δ_y improved as λ gets smaller as illustrated in Figure 28. The ultimate strength (H/H_y) increased by 8% as λ decreased from 0.7 to 0.25 and 2.5% between 0.7 to 0.8 and 1% beyond 0.8. The maximum displacement (δ_m/δ_y) corresponding to maximum strength was increased by 88% (shifted from 0.53 to 1), as λ decreased from 0.7 to 0.25.

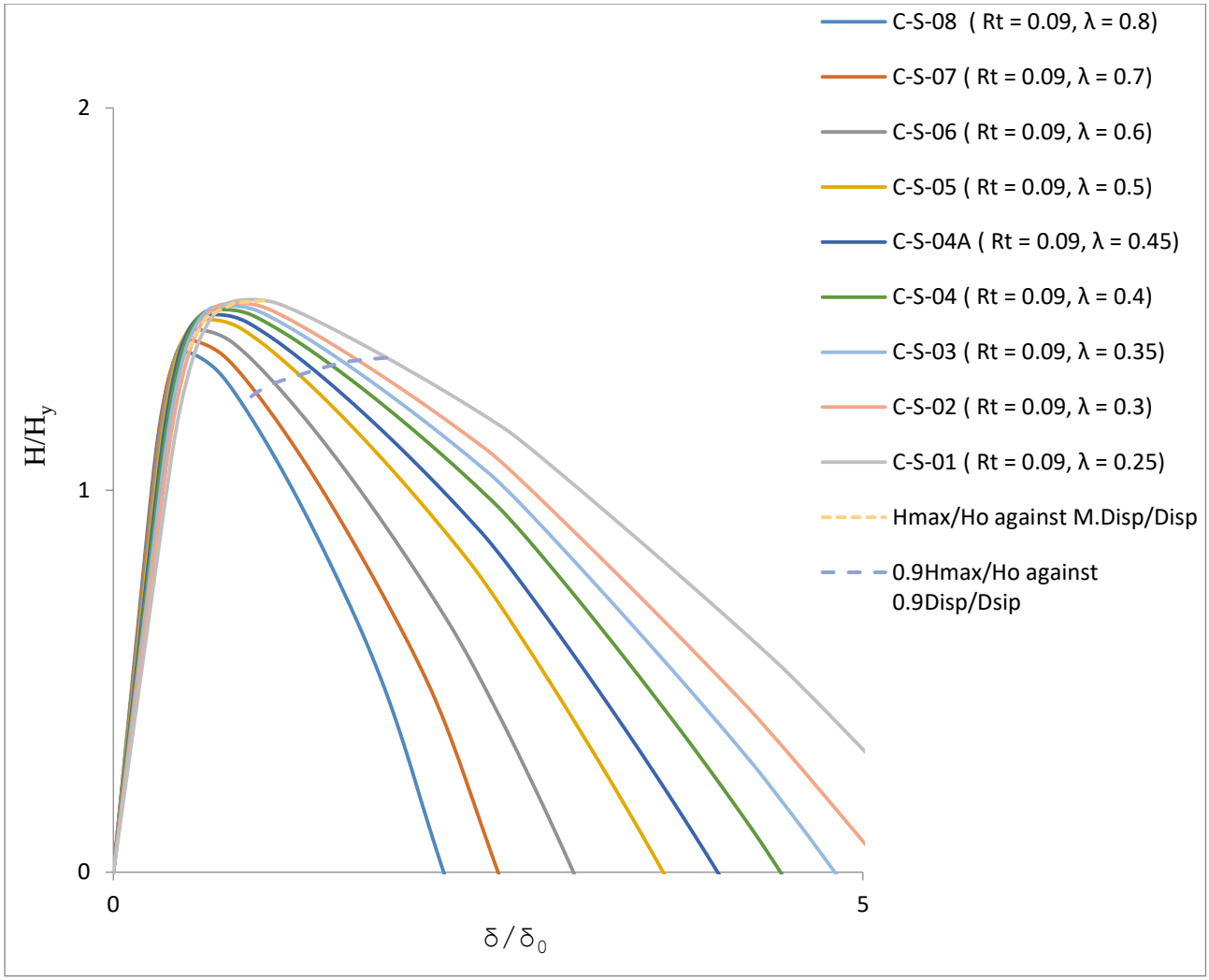

Figure 28: Effect of λ on strength and ductility on circular tubes with diaphragms.

5.3 Deformation

Inspection of Figures 29 (a) and (b) and Figure 30 (a) and (b) shows deformation pattern of the numerically obtained hysteric loops and the formation of a plastic hinge at the base. The elephant budge at the base of the column after formation of the plastic hinge. The amount of bulge and deformation at the base reduced compared with deformation reported in thin walled circular steel columns with no diaphragms. Diaphragms greatly reduced both local and global buckling. The buckling mode indicated a half-sine wave, with inwards and outwards deflections at the positions where the plastic hinge developed.

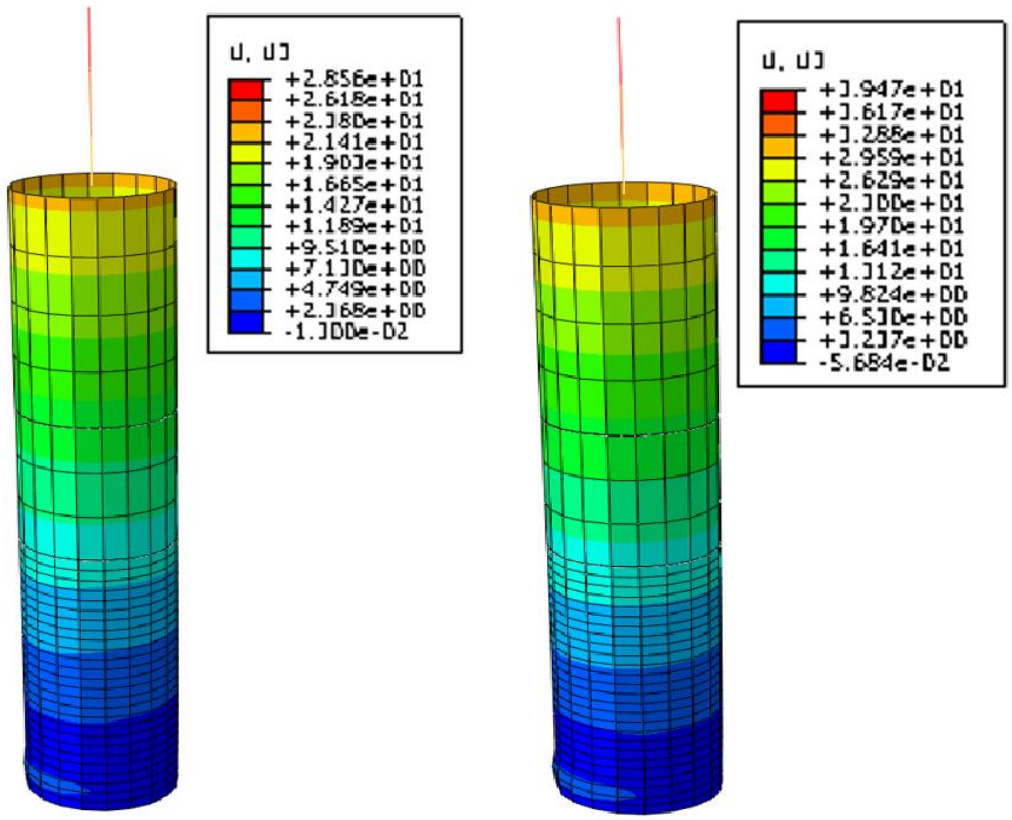

(a) (b)

Figure 29: Deformation at base for columns C-R-08 (a) H_{max}/H_y (b) 0.9 H_{max}/H_y

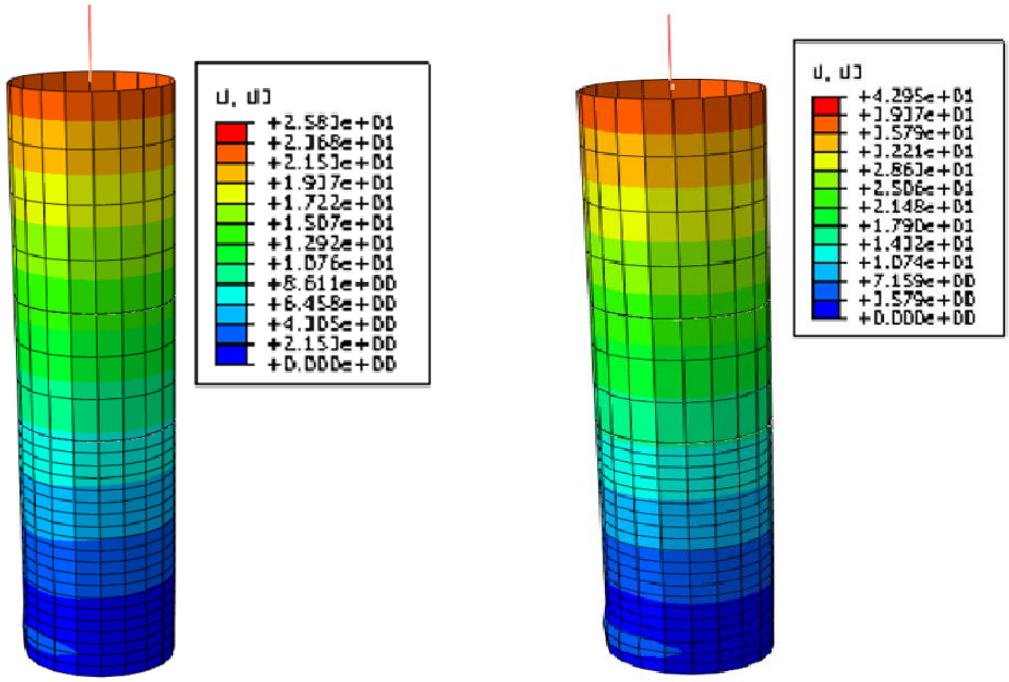

(a) (b)

Figure 30: Deformation at base for columns C-R-04 (a) H_{max}/H_y (b) 0.9 H_{max}/H_y

5.4 Strength and ductility evaluation of prismatic TWCSTC with diaphragms

Table 4 lists the computed ultimate strength and ductility values of the analyzed columns. Figures 31 and 32, indicate H_{max}/H_y plotted against $(1+P/P_y)R_t\lambda$ and $\delta_{0.9}/\delta_y$ plotted against $(1+P/P_y)R_t\lambda$ considering the interaction of R_t, λ and P/P_y on the strength of the column. Equations (5.1) and (5.2) are the proposed relationships obtained by fitting the computed ultimate strength of the uniform TWCSTC and the uniform TWCSTC with diaphragms with the design parameters respectively. The δ_m/δ_y and $\delta_{0.9}/\delta_y$ are key the parameters used to evaluate the ductility performance for both prismatic TWCSTC and prismatic TWCSTC with diaphragms. In addition, the $\delta_{0.9}/\delta_y$ parameter in both pushover and cyclic lateral loading characteristics shows the large displacement possible before sudden drop in strength and failure. Local buckling significantly reduces strength of the columns after peak strength. This, makes it more reasonable to use the $\delta_{0.9}/\delta_y$ parameter to evaluate ductility. The proposed formulae that fitted the computed strength are shown in Equations 5.1 and 5.2:

$$\frac{H_{\max}}{H_y} = \frac{1.13}{[(1+\frac{P}{P_y})R_t\lambda]^{0.07}} \qquad (5.1)$$

$$\frac{H_{\max}}{H_y} = \frac{1.0248}{[(1+\frac{P}{P_y})R_t\lambda]^{0.114}} \qquad (5.2)$$

In addition, the applicable ranges of R_t, λ and P/P_y for developed formulae are $0.06 < R_t < 0.12$, $0.25 < \lambda < 0.6$, and $P/P_y < 0.2$.

Table 4: Strength and ductility of analyzed prismatic TWCSTC and prismatic TWCSTC with diaphragms.

				Strength and ductility ratio (cyclic)			**Strength and ductility ratio (pushover)**		
Column	**H_y (kN)**	**δ_y (mm)**		**H_{max}/H_y**	**δ_m/δ_y**	**$\delta_{0.9}/\delta_y$**	**H_{max}/H_y**	**δ_m/δ_y**	**$\delta_{0.9}/\delta_y$**
P5-e0	232.00	14.00	Analysis	1.46	1.91	3.00	1.46	1.91	3.00
			Test	1.46	1.91	3.00	1.46	1.91	3.00
P1	415.20	10.60	Analysis	1.45	2.40	2.90	1.45	2.40	3.00
			Test	1.45	2.40	2.90	1.41	2.40	2.90
C	414.90	10.60	Analysis	1.45	2.40	3.10	1.45	2.40	3.90
			Test	1.45	2.40	3.10	1.45	2.40	3.90
C-S-000	210.30	1.30	Height less than diaphragm location						
C-S-00	105.00	5.30							
C-S-01	84.10	8.30	Analysis	1.50	1.00	1.82	1.50	1.00	1.82
C-S-02	70.00	12.00	Analysis	1.49	0.81	1.65	1.49	0.81	1.65
C-S-03	60.00	16.40	Analysis	1.48	0.77	1.53	1.48	0.77	1.53
C-S-04	52.60	21.40	Analysis	1.47	0.73	1.45	1.47	0.73	1.45
C-S-04A	46.70	27.10	Analysis	1.46	0.65	1.34	1.46	0.65	1.34
C-S-05	42.00	33.40	Analysis	1.45	0.61	1.25	1.45	0.61	1.25
C-S-06	35.00	48.10	Analysis	1.42	0.57	1.06	1.42	0.57	1.06
C-S-07	30.00	65.50	Analysis	1.39	0.53	0.94	1.39	0.53	0.94
C-S-08	26.30	85.50	Analysis	1.36	0.49	0.86	1.36	0.49	0.86
C-R-01	81.90	26.40	Analysis	1.59	0.89	2.34	1.59	0.89	2.34
C-R-02	69.00	26.60	Analysis	1.55	0.80	1.93	1.55	0.80	1.93
C-R-03	59.50	26.80	Analysis	1.51	0.77	1.66	1.51	0.77	1.66
C-R-04	52.40	27.00	Analysis	1.49	0.77	1.60	1.49	0.77	1.60
C-R-05	46.70	27.06	Analysis	1.46	0.65	1.42	1.46	0.65	1.42
C-R-06	42.20	27.14	Analysis	1.44	0.61	1.18	1.44	0.61	1.18
C-R-07	38.50	27.21	Analysis	1.42	0.61	1.10	1.42	0.61	1.10
C-R-08	35.30	27.27	Analysis	1.40	0.57	0.95	1.40	0.57	0.95
C-R-09	32.70	27.32	Analysis	1.38	0.57	0.90	1.38	0.57	0.90
C-R-10	30.40	27.36	Analysis	1.36	0.53	0.86	1.36	0.53	0.86

5.5 Comparative values for the columns

Table 4, shows an increasing trend of strength and ductility for the columns as R_t and λ decrease. The ultimate strength of the thin walled steel tubular columns with diaphragms is improved when parameter $(1+P/P_y)R_t\lambda$ decreases as shown in Table 5. The failure of the thin-walled steel tubular column was considered to occur when the deformation exceeded δ_m and progressed to $\delta_{0.9}$. The δ_m is the deformation corresponding to H_{max}/H_y, where $\delta_{0.9}$ is the displacement when post-peak strength drops to 90% of H_{max}/H_y after the peak strength. δ_m/δ_y and $\delta_{0.9}/\delta_y$ are the key parameters used to evaluate the ductility performance of the columns and were applied as indicated in this study.

Moreover, the strength of thin-walled circular tubular steel columns decreases significantly after peak due to the influence of local buckling. Therefore, the $\delta_{0.9}/\delta_y$ parameter is more reasonable in the evaluation of ductility. The ductility evaluation plots are shown in Fig. 32 and Fig. 33. Fig. 32; shows the power plot relating $\frac{\delta_m}{\delta_0}$ and$R_t\lambda$. In addition, Fig. 33 shows the power plot relating $\frac{\delta_{0.9}}{\delta_y}$ and $(1+P/P_y)R_t\lambda$. Also, these two figures are curve fitted, and equations 5.3 and 5.4 were determined.

The proposed formulae that fit the computed $\frac{\delta_m}{\delta_y}$ and $\frac{\delta_{0.9}}{\delta_y}$

$$\frac{\delta_m}{\delta_y} = \frac{0.1175}{[(R_t\lambda)]^{0.543}} \qquad (5.3)$$

$$\frac{\delta_{0.9}}{\delta_y} = \frac{0.1085}{[(1+\frac{P}{P_y})R_t\lambda]^{0.812}} \qquad (5.4)$$

In addition, Fig. 31, shows the relationship of the two critical deformation determined in the study. An increase in maximum deformation led to an increase in post buckling deformation.

Equation 5.3 and 5.4 are the interaction equations relating maximum and post buckling deformation and the key design parameters for the prismatic TWCSTC with diaphragms.

Table 5: Strength and ductility comparative parameters

Column	R_t	λ	$(1+P/P_y)*R_t*\lambda$	$R_t\lambda$
C-R-01	0.05	0.45	0.026	0.023
C-R-02	0.06	0.45	0.031	0.027
C-R-03	0.07	0.45	0.036	0.032
C-R-04	0.08	0.45	0.041	0.036
C-R-05	0.09	0.45	0.047	0.041
C-R-06	0.1	0.45	0.052	0.045
C-R-07	0.11	0.45	0.057	0.050
C-R-08	0.12	0.45	0.062	0.054
C-R-09	0.13	0.45	0.068	0.059
C-R-10	0.14	0.45	0.072	0.063
C-S-01	0.09	0.25	0.026	0.023
C-S-02	0.09	0.3	0.031	0.027
C-S-03	0.09	0.35	0.036	0.032
C-S-04	0.09	0.40	0.041	0.036
C-S-04A	0.09	0.45	0.047	0.041
C-S-05	0.09	0.50	0.052	0.045
C-S-06	0.09	0.60	0.062	0.054
C-S-07	0.09	0.70	0.072	0.063
C-S-08	0.09	0.80	0.083	0.072

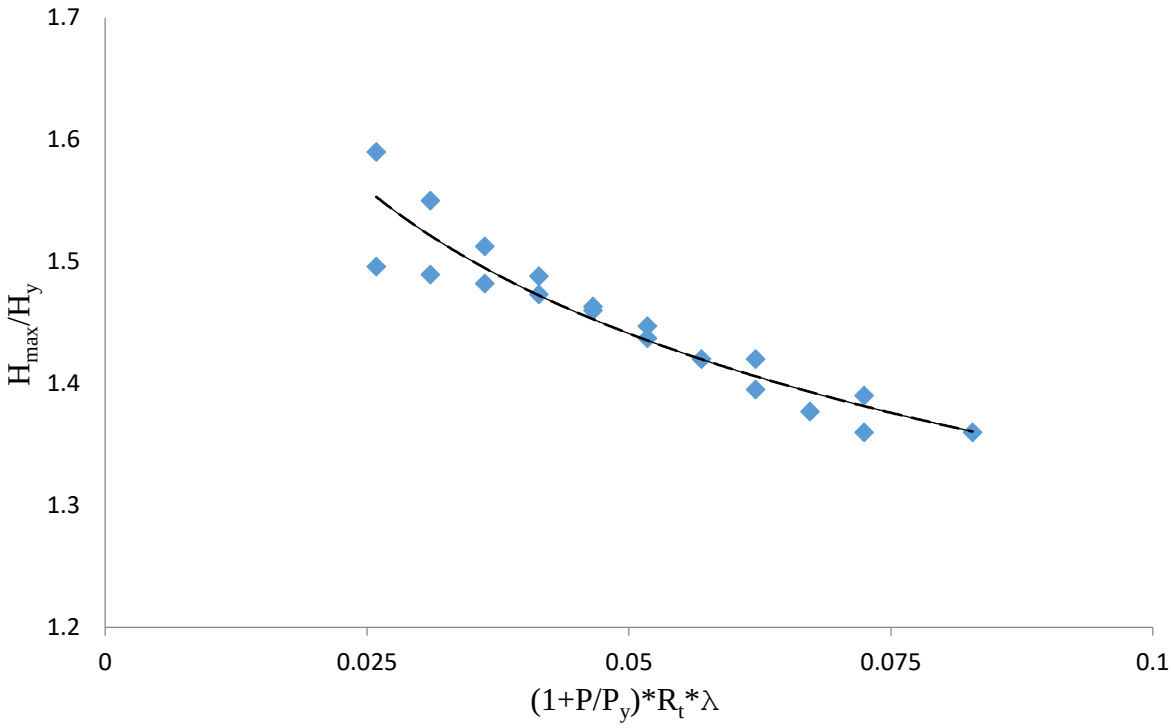

Figure 31: Ultimate strength of the thin-walled circular steel tubular columns.

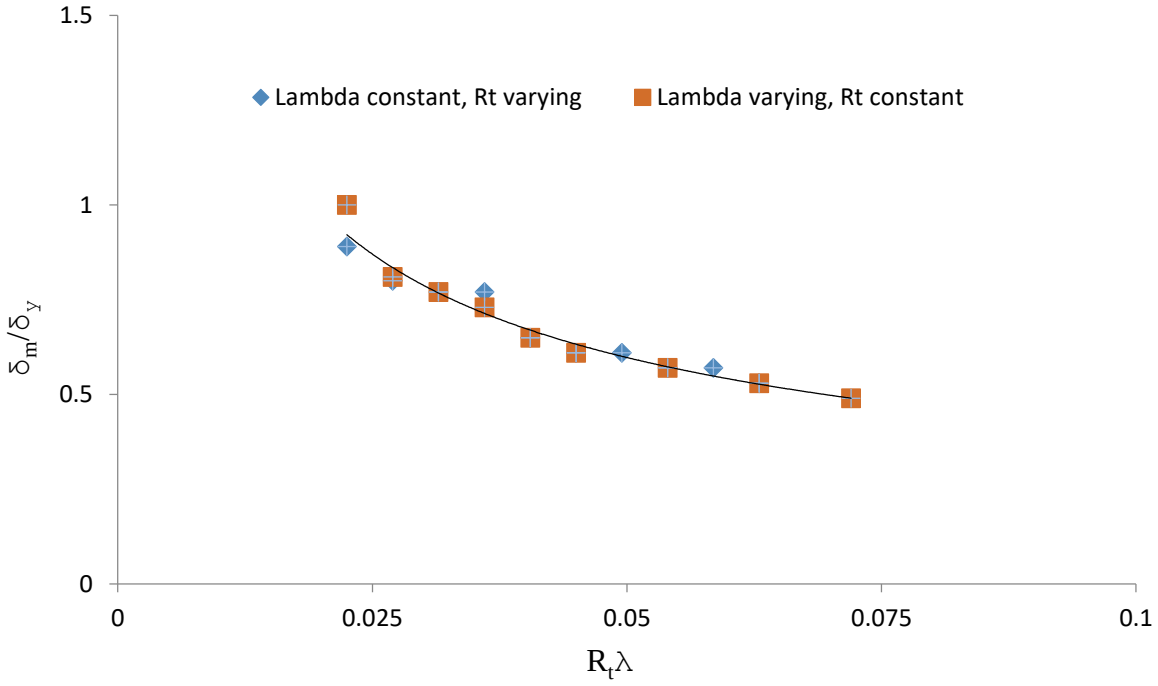

Figure 32: Ductility considering (δ_m/δ_y).

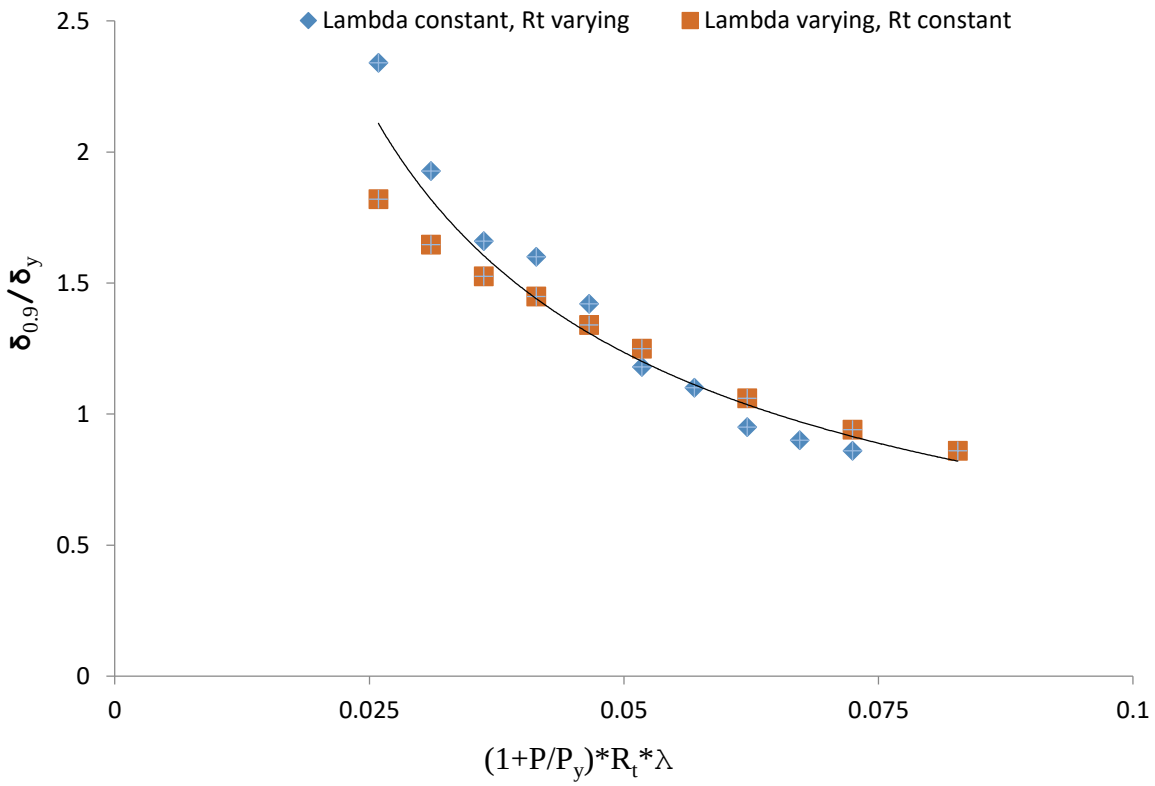

Figure 33: Ductility of considered columns ($\delta_{0.9}/\delta_y$).

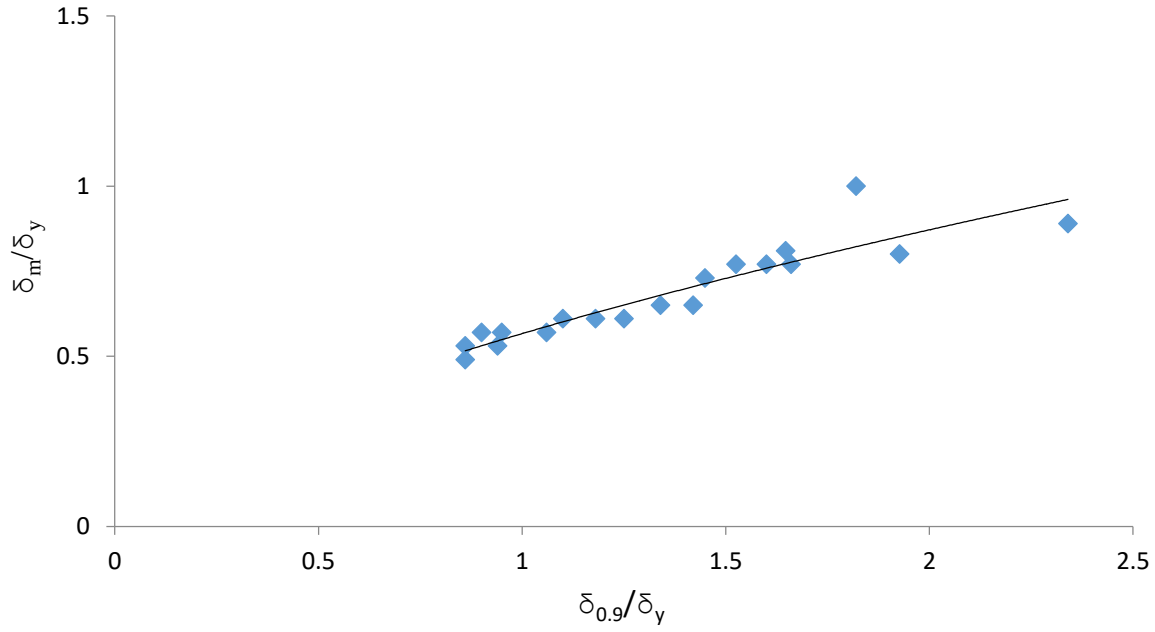

Figure 34: Ductility deformations relationship (δ_m/δ_y and $\delta_{0.9}/\delta_y$).

5.6 Summary

Figures 31, 32, and 33 show the interaction of R_t, λ, P/P_y on the strength, maximum deformation and ductility respectively. The three plots which indicated a curve decreasing from the left to the right were used to develop the interaction design equations.

Figure 34 show the linear relationship between the maximum deformation to the ductility. The increase in the maximum deformation resulted to an increase in the ductility.

CHAPTER 6.

CONCLUSIONS AND FUTURE WORK

6.1 Conclusions

In this research, thin-walled circular tubular steel columns with diaphragms were evaluated for strength and ductility. Diaphragms increased both strength and ductility as compared to their counterpart uniform thin-walled circular steel tubular columns.

R_t and λ are the design key parameters that control local buckling and flexural buckling in thin-walled circular steel tubes. Appropriate ranges of R_t and λ were computed and this would help in achieving a cost-effective and safe design. The columns with smaller R_t and λ absorbed more energy and provided higher ductility than the columns with larger R_t and λ. A series of proposed relationships to predict the ultimate strength, maximum displacement and ductility of the thin-walled circular tubular steel columns were provided.

The ultimate strength (H_{max}/H_y) improved by 10% as R_t decreased from 0.12 to 0.06 and 1% for the R_t values above 0.12 and also the ultimate strength (H_{max}/H_y) was increased by 8% as λ decreased from 0.7 to 0.25 and 2.5% between 0.7 to 0.8 and 1% beyond 0.8. It can be summarized that R_t values smaller than 0.05 and higher than 0.12 and λ values smaller than 0.25 and higher than 0.8 does not give the columns any strength increases and would not make economic reason to use diaphragms.

The proposed ultimate strength and ductility equations involving interaction on radius-to-thickness ratio, column slenderness ratio, and axial load ratio are expected to be useful for the practical design of thin-walled steel circular tubular columns.

This study confirmed diaphragm's improved the strength and the ductility of the thin-walled steel circular tubular columns.

6.2 Recommendation

The interaction design equations for the key design parameters R_t and λ were determined considering constant thickness of the diaphragm. Additional research that considers different values of thickness of the diaphragms is therefore recommended.

Secondly, partly filled circular concrete steel columns should be considered and monitor the effect of concrete on the interaction formulae that relates R_t, λ and P/P_y.

6.3 Future Work

This research observed great improvement in the strength and the ductility after addition of two diaphragms' on thin-walled circular steel tubular columns. However, buckling near the base of the columns was still noticed. The next phase of this research will consider partly filling the thin-walled circular steel tubular columns with concrete up to the height level where buckling was noticed during modelling; a height equal to (D_0-$2D_0$). Then, interaction equations that relate R_t, λ and P/P_y will be determined and proposed.

REFERENCES

Al-Kaseasbeh, Q., & Mamaghani, I. H. P. (2019a). Performance of Thin-Walled Steel Tubular Circular Columns with Graded Thickness under Bidirectional Cyclic Loading. *Structures Congress 2019*, 1–10. https://doi.org/10.1061/9780784482230.001

Al-Kaseasbeh, Q., & Mamaghani, I. H. P. (2019b). Buckling strength and ductility evaluation of thin-walled steel stiffened square box columns with uniform and graded thickness under cyclic loading. *Engineering Structures*, *186*, 498–507. https://doi.org/10.1016/j.engstruct.2019.02.026

Al-Kaseasbeh, Q., & Mamaghani, I. H. P. (2019c). Thin-Walled Steel Tubular Circular Columns with Uniform and Graded Thickness under Bidirectional Cyclic Loading. *Thin-Walled Structures*, *145*, 106449. https://doi.org/10.1016/j.tws.2019.106449

Aoki, T., & Susantha, K. A. S. (2005). Seismic Performance of Rectangular-Shaped Steel Piers under Cyclic Loading. *Journal of Structural Engineering*, *131*(2), 240–249. https://doi.org/10.1061/(ASCE)0733-9445(2005)131:2(240)

Dalia, Z. M., Bhowmick, A. K., & Grondin, G. Y. (2021). Local buckling of multi-sided steel tube sections under axial compression and bending. *Journal of Constructional Steel Research*, *186*, 106909. https://doi.org/10.1016/j.jcsr.2021.106909

Esper, P., & Tachibana, E. (1996). Lessons Learned from Kobe Earthquake. *Geological Journal*.

Fukumoto, Y., Uenoya, M., & Nakamura, M. (2003). Cyclic performance of stiffened square box columns with thickness tapered plates. *Steel Structures*, *3*, 107–115.

Gao, S., Usami, T., & Ge, H. (2000). Eccentrically Loaded Steel Columns under Cyclic In-Plane Loading. *Journal of Structural Engineering*, *126*(8), 964–973. https://doi.org/10.1061/(ASCE)0733-9445(2000)126:8(964)

Ge, H., Gao, S., & Usami, T. (2000). Stiffened steel box columns. Part 1: Cyclic behaviour. *Journal of Engineering Structures*, *29*, 1691–1706.

Goto, Y., Ebisawa, T., & Lu, X. (2014). Local Buckling Restraining Behavior of Thin-Walled Circular CFT Columns under Seismic Loads. *Journal of Structural Engineering*, *140*(5), 04013105. https://doi.org/10.1061/(ASCE)ST.1943-541X.0000904

Goto, Y., Wang, Q., & Obata, M. (1998). FEM Analysis for Hysteretic Behavior of Thin-Walled Columns. *Journal of Structural Engineering*, *124*(11), 1290–1301. https://doi.org/10.1061/(ASCE)0733-9445(1998)124:11(1290)

Hibbit, K., & Sorensen. (2014). *Abaqus 2014 Documentation; 2014.*

Kazuhiro Nishikawa, Satoshi Yamamoto, Tohru Natori, Keiji Terao, Hiromichi Yasunami, & Masahiro Terada. (1998). Retrofitting for seismic upgrading of steel bridge columns. *Engineering Structures*, *20*(4–6), 540–551. https://doi.org/10.1016/S0141-0296(97)00025-4

Kwon, Y. B., Kim, N. G., & Hancock, G. J. (2007). Compression tests of welded section columns undergoing buckling interaction. *Journal of Constructional Steel Research*, *63*(12), 1590–1602. https://doi.org/10.1016/j.jcsr.2007.01.011

Li, H., Gao, X., Liu, Y., & Luo, Y. (2017). Seismic performance of new-type box steel bridge piers with embedded energy-dissipating shell plates under tri-directional seismic coupling action. *International Journal of Steel Structures*, *17*(1), 105–125. https://doi.org/10.1007/s13296-015-0192-z

Lyu, F., Goto, Y., Kawanishi, N., & Xu, Y. (2020). Three-Dimensional Numerical Model for Seismic Analysis of Bridge Systems with Multiple Thin-Walled Partially Concrete-Filled Steel Tubular Columns. *Journal of Structural Engineering*, *146*(1), 04019164. https://doi.org/10.1061/(ASCE)ST.1943-541X.0002451

Mamaghani, I. H. P. (1996). *Cyclic Elasto-Plastic Behaviour of Steel Structures: Theory and Experiment.* [PhD dissertation]. University of Nagoya, Nagoya, Japan.

Mamaghani, I. H. P. (2008). Seismic Design and Ductility Evaluation of Thin-Walled Steel Bridge Piers of Box Sections. *Transportation Research Record: Journal of the Transportation Research Board*, *2050*(1), 137–142. https://doi.org/10.3141/2050-14

Mamaghani, I. H. P., Khavanin, M., Erdogan, E., & Falken, L. (2008). Elastoplastic Analysis and Ductility Evaluation of Steel Tubular Columns Subjected to Cyclic Loading. *Structures Congress 2008*, 1–12. https://doi.org/10.1061/41016(314)298

Mamaghani, I. H. P., & Packer, J. A. (2002). *Inelastic behavior of partially concrete-filled steel hollow sections*. 1–9.

Mamaghani, I. H. P., Usami, T., & Mizuno, E. (1997). Hysteretic behavior of compact steel box beam-columns. *Journal of Structural Engineering*, *43*, 187–194.

Mustafa, S. A. A., Elhussieny, O. M., Matar, E. B., & Alaaser, A. G. (2018). Experimental and FE analysis of stiffened steel I-column with slender sections. *Ain Shams Engineering Journal*, *9*(4), 1635–1645. https://doi.org/10.1016/j.asej.2016.12.001

Serras, D. N., Skalomenos, K. A., Hatzigeorgiou, G. D., & Beskos, D. E. (2016). Modeling of circular concrete-filled steel tubes subjected to cyclic lateral loading. *Structures*, *8*, 75–93. https://doi.org/10.1016/j.istruc.2016.08.008

Ucak, A., & Tsopelas, P. (2012). Accurate modeling of the cyclic response of structural components constructed of steel with yield plateau. *Engineering Structures*, *35*, 272–280. https://doi.org/10.1016/j.engstruct.2011.10.015

Watanabe, E., Sugiura, K., & Oyawa, W. O. (2000). Effects of multi-directional displacement paths on the cyclic behaviour of rectangular hollow steel columns. *Doboku Gakkai Ronbunshu*, *2000*(647), 79–95. https://doi.org/10.2208/jscej.2000.647_79